Photovoltaic Charge Station on Garage Roofs with Passive Reflectors

By
Aylin ÇANTAY

A Dissertation Submitted to the
Graduate School in the Partial Fulfilment of the
Requirements for the Degree of

MASTER OF SCIENCE

Department: Energy Engineering
Major: Energy Engineering (Energy and Power Systems)

Izmir Institute of Technology
Izmir, Turkey

September, 2000

We approve the thesis of Aylin ÇANTAY

Date of Signatura

.....

28.09.2000

Prof. Dr. Gürbüz ATAGÜNDÜZ

Supervisor

Department of Energy Engineering

.....

28.09.2000

Assoc.Prof.Dr. Mehmet GÜNEŞ

Co-Supervisor

Department of Physics

.....

28.09.2000

Prof. Dr. Zafer İLKEN

Department of Mechanical Engineering

.....

28.09.2000

Prof. Dr. Necdet ÖZBALTA

Ege University, Solar Energy Institute

.....

28.09.2000

Prof.Dr.Gürbüz ATAGÜNDÜZ

Head of interdisiplinary

Energy Engineering Program

ACKNOWLEDGMENT

I would like to thank and express my deepest gratitude to Prof. Dr. Gürbüz Atagündüz for understanding, help and encouragement during this study and in the preperation of this thesis.

I also would like to thank Res. Ass. Fatih Bacaksız for his help on design of construction.

Finally, I would like to thank my husband and my family for their help, support and patience.

Aylin Çantay

September 2000 Cankaya/IZMIR

ABSTRACT

This study involves a photovoltaic charge station which could be placed on garage roofs in order to charge the battery of an electrical car. The aim of this thesis is to design an efficient photovoltaic charge station and construction of omega type solar charge station. That's why various models were designed and calculated amount of energy.

A photovoltaic charge station has 16 photovoltaic modules with dimensions 1293 mm*329 mm*34 mm. In this study five different type of solar charge stations were compared. These are, omega type solar charge station (first type), south facing type solar charge station with different angles (second type), south facing type solar charge station with fixed angles (third type), inverse of omega type solar charge station (fourth type), optimisation of south facing type solar charge station with different angles (fifth type). After calculating of collected solar energy, the fifth type solar charge station was chosen as the most efficient solar charge station.

After these theoretical calculations, omega type solar charge station has been installed on the Electrical Engineering Department's roof. Voltages and current intensitiesof omega type solar charge station were measured from 28 June 2000 to 15 October 2000 in order to determine the solar power obtained and to compare it with the calculated values and measured data by Solar Energy Institute of Aegean University and meteorological station in Güzelyalı. The results obtained are satisfactory.

ÖZ

Bu çalışma, elektrikli arabaların akü şarjı için garaj çatılarına kurulacak olan fotovoltaik şarj istasyonlarını içermektedir. Bu tezin amacı, en verimli olan güneş şarj istasyonunun dizaynı ve elde edilen enerji miktatrının hesaplanmasıdır.

Bir fotovoltaik şarj istasyonu 1293 * 329 * 34 mm boyutlarında olan 16 adet fotovoltaik pilden meydana gelmiştir. Bu çalışmada beş değişik güneş şarj istasyonu karşılaştırılmıştır. Bunlar, omega tipi güneş şarj istasyonu (birinci tip), güneye bakan değişik eğimli modüller (ikinci tip), güneye bakan sabit eğimli modüller (üçüncü tip), omega tipi güneş şarj istasyonunun tersi (dördüncü tip) ve güneye bakan değişik eğimli modüllerin optimizasyonudur (beşinci tip). Toplanan güneş enerjisi miktarlarının hesaplanmasından sonra güneye bakan değişik eğimli modüllerin optimizasyonu olan güneş şarj istasyonu en uygun model olarak seçilmiştir.

Bu teorik hesaplamardan sonra, omega tipi güneş şarj istasyonunun konstrüksüyonu yapıldı. 28 Haziran 2000'den 15 Ekim 2000'e kadar voltaj ve elektrik akım yoğunluğu ölçüldü. Bu ölçümler doğrultusunda, omega tipi güneş şarj istasyonunun gücü hesaplandı ve daha önce hesaplanan değerlerle, Ege Üniversitesi Güneş Enerjisi Enstitüsü'nden alınan ölçülmüş değerlerle ve Güzelyalı Meteoroloji istasyonundan alınan değelerle karşılaştırıldı. Elde edilen sonuçlar memnun edicidir.

TABLE OF CONTENTS

LIST OF FIGURES

LIST OF TABLES

Chapter I

INTRODUCTION

As the world population increases, so does the demand for transportation. Automobiles, being the most common means of transportation are one of the main sources of pollution. Today, 95% of energy requirement of automobiles is supplied from petroleum products. Cars contribute anywhere from 60%-90% of all air pollution. Every gallon that car uses makes 22 pounds of carbon dioxide, which in turns adds to the greenhouse effect and other hazards like air pollution. The carbon dioxide found in the atmosphere accounts for 30% of the overall pollution caused by transportation (3). According to the World Energy Council Turk National Committee's data in 1993, petroleum reserves are known as 136.7 billion tons. However, we know that these reserves will be consumed in 43.1 years (29). That's why scientists try to find new technologies for transportation with zero emission like electrical vehicle

The first electric car was built in Scotland in 1837 by Robert Davidson. Electric vehicles were widely produced in the 1800's when the lead acid battery was perfected. First production electric car created a sensation when exhibited in Chicago in 1892. Belgian built electric racing car "La Jamais Contente" (never satisfied) set a world land speed record of 68 mph in 1899. Twenty companies were producing 6000 electric vehicles and trucks per a year in 1913. Oil embargo in 1973 and resurgence of interest in electric vehicles. In 1977 Japan had 13000 electric vehicles in operation, Great Britain had 70000 and United States had 3000 with projections of 25 million by the year 2000. Gas prices were than lowered and electric car declined again (26).

Solutions for many of such conditions as these make industry towards alternative fuelled vehicles. An alternative fuelled vehicle is vehicle that relies an energy other than gasoline, and can either be zero or lower emission. Although solar and electric vehicles have the potential to reduce harmful pollutants.

In order to evaluate the applying of solar vehicles, one must understand the fundamental principles governing solar vehicles, which rely on photovoltaic cell.

Joining p-type and n-type semiconductors creates a photovoltaic cell. When they are brought together, electron carries are free to move around. Since the have opposite

charges, carriers move toward each other. In the process they from an electric field called a "gradient", similarly to the electric field formed within a parallel plate capacitor. This electric field is also responsible for the direction of the electric current.

Solar energy is produced when sunlight strikes the photovoltaic cell. Atoms are stormed by photons and forced to give up electrons. These negative electrons together with the positive electrons the leave behind travel down the gradient. In the process an electric current is formed and sent down one side to a circuit and back to the other side. This energies any electrical or battery found along way (26).

The advantages of solar energy start with the fact that the sun is environmental sound. The production of solar energy by solar car does not any harm to the environment. Solar cars are emission free and do not deplete any of the Earth's natural resources. After all, they use a resource that is not even on Earth. This leads to the second advantage, sunlight is free. To use sunlight to power vehicles does not cost the consumer anything. Since no ones own the sun, the consumer does not have to worry about paying for gas or electricity. The third advantage of solar cars is that the energy supply is locally produced. This is good, because in some places it is hard to bring electricity or any other conventional means of producing energy to. In process there is no gas or power lines solar energy would be most useful. The last advantage of solar cars have is that solar power is generated during peak demand for energy. Most people do the majority of their driving during the day, which is the peak time for electricity production. These advantages put together would certainly outweigh the cost of overcoming the obstacles of solar cars and give a great outlook to future of solar powered vehicles.

In this study, the models of solar charge station will be researched which could be placed on garage roofs in order to charge the battery of an electric car. But they have small action radius, in general about 80 km. Therefore, their batteries must be charged daily. A photovoltaic charge station has 16 photovoltaic modules with dimensions 1293mm*329mm*34mm. Here, five different type of solar charge station will be compared. These are omega type solar charge station, south facing solar charge station with different angles, south facing solar charge station with fixed angles, inverse of omega type solar charge station, optimisation of south facing solar charge station with different angles. Amount of collecting energy will be calculated for each type solar

charge station as monthly with different angles. According to the results, the diagrams will be plotted amount of energy - months. At the end of this study, the most stable and the most efficient energy collecting solar charge station will be chosen.

Chapter II

THE SUN

The sun is a "more or less average" star with a mass equal to nearly one-third of a million Earths (11). Spectral measurements have confirmed the presence of nearly all the known elements in the sun. As is typical of many stars, about 94 % of the atoms and nuclei in the outer parts are hydrogen, about 5.9 % are helium, and a mixture of all the other elements make up the remaining one-tenth of one percent (22). A gaseous globe with a radius of $7*10^5$ km, it has a mass about $2*10^{30}$ kg. This grater than the earth's mass by a factor of about 330000. The total rate of energy output from the sun $3,8*10^{33}$ ergs/s ($3,8*10^{23}$ kW). At a mean distance of $1,496*10^8$ km from the sun, the earth intercepts about 1 part in 2 billion of this energy (11). One proposed solar structure is shown in Figure1.

The sun gets its energy from the fusion reaction of two hydrogen nuclei joining together to make one helium nucleus. This is the same reaction as that of the hydrogen bomb. The fusion reaction began a few billion years ago as a result of the great temperatures in the sun's center caused by the gravitational contraction of the huge mass of hydrogen gas from which the sun probably formed (20).

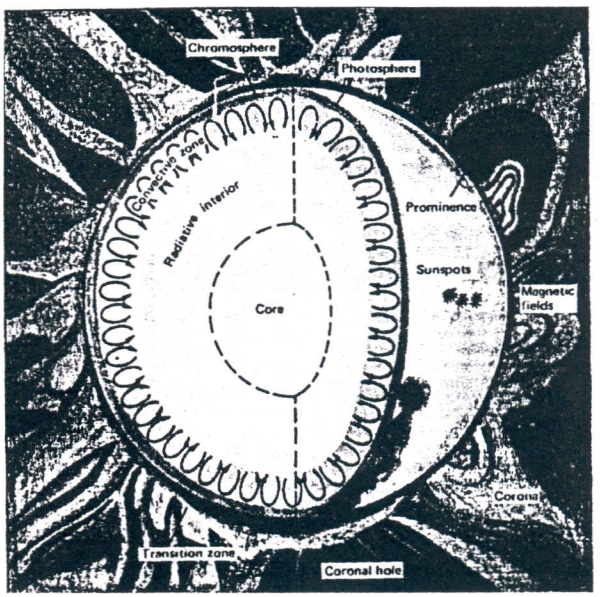

Figure 1: Cross-section of the sun, schematically

Most of the energy produced in the fusion furnace of the sun transmitted radially as electromagnetic radiation popularly called sunshine or solar energy. The sun radiates at an effective surface temperature about 5800 K (11).

The sun's relatively small core is hot about 25000000 F and it is in the core that the fusion reaction occurs. Eventhough the sun's energy output is small compared to its huge size; it turns out energy on an enormous scale by Earth's standards, some 10 million megatons of energy per seconds (20). An additional, relatively small amount of energy reaches earth through the process of conduction. Energetic particles from the sun strike other particles, heat them and they in turn heat others. Solar storms in the lower atmosphere of the sun also shoot streams of energetic particles directly from the photosphere into the atmosphere of the earth. This convective transfer of energy, and the conduction, account for less than a millionth of the energy radiated from the sun (11).

Man sees only the glowing surface of the sun. During solar eclipses when the main disc of blotted out, one can also see the solar atmosphere or corona. The corona is made up of ionised hydrogen, a hydrogen atom with its one electron knocked off. However, the corona also contains all of the elements common on earth (21).

The corona is much more diffuse than the rest of the sun and much hotter that the surface 2000000 K justs above the sun's surface. This corona is thought to extend in diffuse form to the cuter limits of the solar system. Even during quiet periods of the sun, there are coronal streamers of every hot gas out to ten solar diameters. The sun's diameter is 864000 miles (21).

The surface of the sun is covered with bright granules, but the most noticeable features are the sunspots, darker and cooler regions about 4500^{0}C. Sunspots have tremendous magnetic fields, 3000 or 4000 Gauss compared with about one Gauss for the rest of the sun's surface (21).

Sunspots are believed to be places where doughnut-shaped magnetic fields emerge from the sun's surface, and they usually occur in pairs of opposite magnetic polarity. At the maximum solar activity in 1947, a sunspot of five billion square miles was seen (21).

The sun alternates from very quiet to very turbulent and active, then back to quite over 11-year cycles. At the peak of the cycle, numerous solar flares occur which throw out huge masses of the hot gas and energetic particles. These masses of heat,

ionised hydrogen hit the earth's magnetic field, bend it out of shape, disrupt radio communications, cause the aurora borealis, and feed the Van Allen radiation belts (21). Flares are 1000 to 100000 times more dense than the surrounding material on the solar surface, the corona around the flares gets four times hotter than normal, and gas thrown out travels around 2250000 mph. The cause of flares is not known, but they are generally believed to be related to sunspot magnetic fields (21). Flares include luminous and ultraviolet radiations, and may also be accompanied by bursts of X-rays, radio frequency waves, and high-energy charged particles. These particles may have velocities as high as 100000 km/s (14).

In addition to flares, the sun constantly throws out ionised hydrogen in the solar wind. This material moves at nearly one million mph and contains one to ten particles per cubic centimetre. This is still more diffuse than "hardest" vacuum yet made on earth (21).

Chapter III

PHOTOVOLTAIC SYSTEMS

As fossil fuels reserves dwindle, much of many worlds now look to technology and science to provide and new sources of energy. Luckily some hopeful technologies have emerged that will help to wean the world from the sources it has relied on since the industrial revolution. Renewable energy is finally becoming a viable option for countries both countries wanting to switch to cleaner sources of energy as well as developing which are opting to incorporate such sources of energy into their infrastructure initially. While most people are familiar with the capacity of solar energy, to heat water, many are not familiar with a technology that allows the production of electricity through a conversion the sun's energy into atomic energy (5).

The photovoltaic (PV) effect was discovered in 1839 by Edmond Becquerel. For a long time it remained a scientific phenomenon with few device applications. After the introduction of silicon as the prime semiconductor material in the late 1950s, silicon photovoltaic diodes become available. They were soon indispensable for supplying electrical power to telecommunications equipment in remote locations and to satellites. Then, in the 1970s, a major reorientation took place in the general perception of the energy supply problem. The oil crisis of 1973 led to a general public awareness of the limitation of fossil fuels, many governments (including those of the United States, Japan and several European countries) started a few years later, ambitious programs in the search for alternative energy sources, including photovoltaic solar energy. This trend was reinforced by public controversy over nuclear fusion reactors and by series of accidents in nuclear power stations, especially those of Three Mile Island (in 1979) and Chernobyl (in 1986) (25).

Since the beginning of the 1990s, ecological considerations linked with the CO_2 global warming problem have taken over as a main driving force in promoting alternative energy sources, in particular, photovoltaic solar energy. The past two decades have seen constant and substitutional progress in the field of photovoltaic modules commercial prices of modules (when purchased in large quantities) have shown a sustained average reduction of 7.5% per year during the same time, the worldwide

production of modules has increased on average by 18% per year. Although these two trends can be expected to continue in the near future, it will take many decades before photovoltaic modules can substantially contribute to electricity generation. The reduction in photovoltaic module cost progress with the increase of production, but we are rapidly reaching a stage where a further decrease in cost is conditional on the global availability of raw materials. Thus, photovoltaic technologies that involve the use of lesser quantities of cheaper and less refined input materials are favoured (25).

Photovoltaic cells by themselves do not provide sufficient power for utility applications. Individual cells must be interconnected in series and in parallel to achieve desired levels of current or voltage. Groups of cells, when environmental packaged in convenient size for use in the field. Most commercially available modules are generally less than a square meter in size and deliver between 50 and 150 watts. Recently, larger modules with areas of approximately $2.2m^2$ have become available (11).

The most normal configuration for solar cell is to make a p-n junction semiconductor as shown schematically in Figure 2 The junction of the "p-type" and "n-type" materials provides an inherent electric field, which separates the charges created by the absorption of sunlight. This p-n junction is usually obtained by putting a p-type base material into a diffusion furnace containing a gaseous n-type dopant such as phosphorous and allowing the n dopant to diffuse into the surface about 0.2 μm. The junction is thus formed slightly below the planar surface of the cell and the light impinges perpendicular to the junction.

The positive and negative charges created by the absorption of photons are thus encouraged to drift to the front and back of the solar cell. The back is completely covered by a metallic contact to remove the charges to the electrical load. A fine grid of narrow metallic fingers aids the collection of charges from the front of the cell. The surface coverage of the conduction collectors is typically about 5 percent in order to allow as much light as possible to reach active junction area. An antireflective coating is applied on the top of the cell (6).

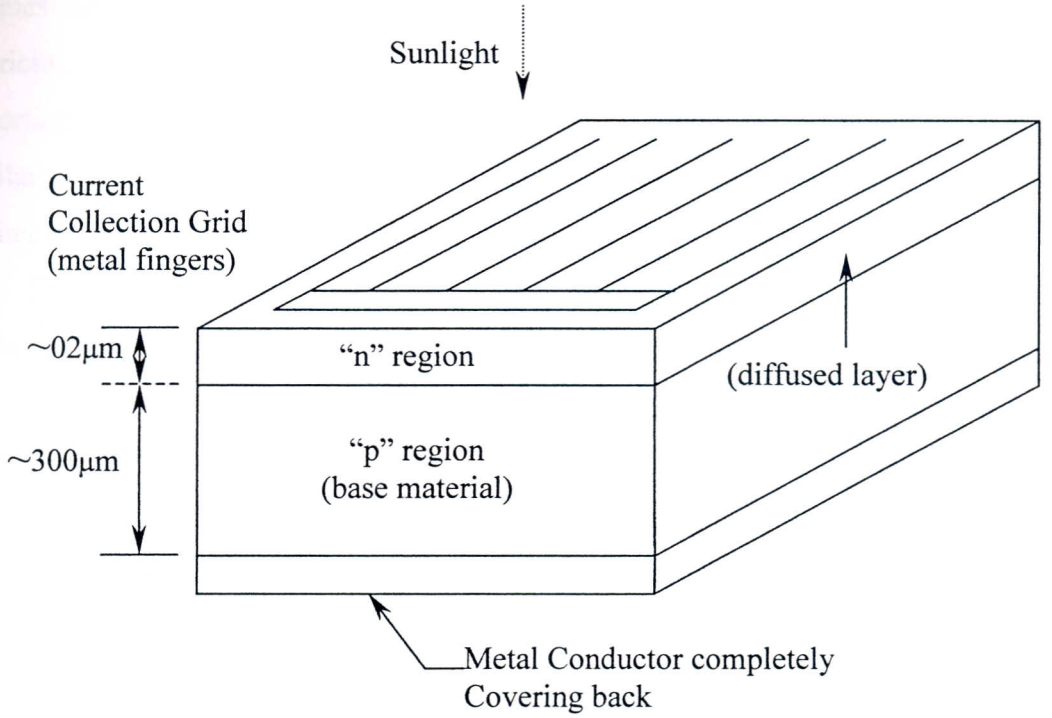

Figure 2: Cross-sectional View of Typical p-n junction cell

The world market for photovoltaic was 57.9 MW in 1992, having increased from less than 1 MW in 1978. Current uses of photovoltaic modules include the followings:

- Lightning (eg. street lights, highway signs, homes)
- Electricity for facilities in remote locations (eg. refrigeration in remote health clinics or homes)
- Communications (eg. telephone, radio communications, emergency call boxes)
- Water pumping (eg. village water supply, irrigation and draining)
- Warning signals (eg. railroad signals)
- Monitoring at remote sites (eg. seismic recording, meteorological information)
- Cathodic protection (eg. preventing corrosion of pipelines, bridges and buildings)
- Battery charging for vehicles (16)

The present cost of electricity from photovoltaic installations is generally (except in remote areas) about an order of magnitude higher than current commercial prices of electricity generated by hydraulic and nuclear power and fossil fuels. Because of physical reasons, it appears at present to be very difficult to substantially increase the energy conversion efficiency of low-cost photovoltaic modules over 15%. Thus, it

becomes necessary to reverse large surfaces for the photovoltaic generation of electricity, which also means the costs of substrates, encapsulations, wiring and supporting structures are decisive factors in the cost break-up of photovoltaic solar installations. This requires a full integration on photovoltaic installations into the existing environment and habitat (25).

Photovoltaic systems offer numerous advantages to utilities. Photovoltaic systems are modular, lightweight, portable and highly reliable. Easily erected in remote areas without expensive support equipment, they require short construction times. Systems are easily removed and leave little or no lasting impact on the environment. They are environmental attractive in that they require no fuel or water, generate no air or water pollution, are noise free and eliminate transmission lines.

Although solar cells and photovoltaic installations do not generate any CO_2 during their operation, they do, however, consume considerable amounts of energy and cause the generation of CO_2 and certain pollutants during their manufacture. The energy payback time (about 3,5 year) and the ecological balance sheet of solar modules and photovoltaic installations are, therefore, important issues to be considered when choosing a future technology.

3.1. How Solar Cells Work

A solar cell is a photovoltaic semiconductor device that converts solar energy directly into electrical energy, see Figure 3. Photons of solar radiation impinging on the cell impart energy to the semiconductor material, cause electrons to flow across a semiconductor junction, usually called p-n junction, and thus convert the solar energy into electrical energy. At present, most solar cells are manufactured from silicon. A single crystal of pure silicon is first grown and then sliced into wafers approximately 0.05 cm thick. Introducing impurities into the raw silicon produces the n and p junctions of the solar cell. The silicon wafer can be made to conduct either negative (n) or positive (p) charges. Arsenic, phosphorous or antimony impurities create an n-type wafer, whereas boron makes the material a p-type carrier. These wafers are arranged in a module to yield the desired current and voltage. When a photon strikes a p-n junction, a negative and a positive charge are created and an electron moves toward the n-type

region, initiating an electric current. By connecting contacts and leads to the surfaces of the wafer, a circuit is formed that allows electrons to return to the p-type region through an external load If the load resistance is small, the cell acts like a constant current generator with the current output equal to the short circuit current. In this region the current output is approximately proportional to the intensity of radiation incident on the cell. But as the load resistance is increased, the cell current decreases and more current flows through the internal diode. For every large values of the load resistance, the voltage across the cell terminals approaches the open circuit voltage. (13)

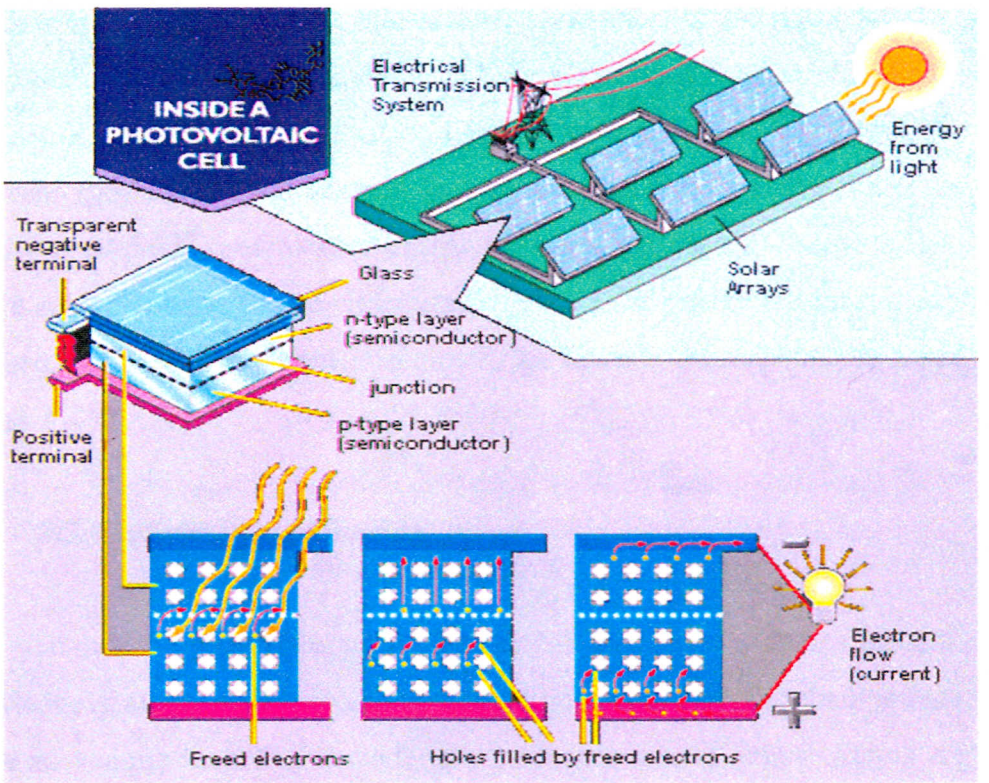

Figure 3. Production of Electricity from the Sun with Photovoltaic Devices

Under standard test conditions of 1000 W/m^2 insolation and a cell temperature of 27^0 C, the short circuit current is approximately 1 to 1.2 A per square centimetre of cell and the open circuit voltage is between 0.55 and 0.6 V. The open circuit voltage is determined primarily by the cell temperature. It decreases at the rate of 0.022 $V/^0C$. The standard test conditions used in terrestrial solar applications were chosen because they

are easy to obtain in production testing. Since, on a clear day, the solar intensity is about 1000 W/m^2 and the average temperature is 27 ^0C, they also yield useful results for actual cell operation. (13)

The basic unit of the photovoltaic system is the module. To build a module, individual cells are assembled in series and/or parallel combinations. The number of cell in series determines the module voltage and the number in parallel determines the module current capability. Modules are assembled together in a frame or support to form an array. (13)

A typical photovoltaic conversion system consists of arrays of solar cells, which may be either flat or combined with solar concentrators mounted to face the sun, plus power conditioning equipment and storage capabilities if necessary for the particular application. The mount may be stationary or may be track the sun. Solar cell arrays are arranged in series or parallel to attain a desired voltage and current output. A controller maintains the required voltage and the resistance of the load determines the current. Usually a battery is used to store energy for use when the sun is down. The dc output from a solar cell array can be either used to charge the battery or transmitted directly to the load. When an ac output is required, an inverter must be incorporated into the system. (13)

3.2. Electricity from the Sun

In order to understand what electricity is and where it comes from, some basic knowledge of atoms is required. Everything around you, from the chair you are sitting in to the air you are breathing is made up of arrangements of atoms. Atoms are so small that's why they can not be seen even with a regular microscope. You could fit billions on the head of a pin. Atoms are the fundamental building blocks of all matter on the smallest scale imaginable. But even atoms have their own structures consisting of a nucleus and a number of electrons. (5)

An atom can be visualised as a small sphere inside of a larger sphere, looking much like a ping pong ball inside center of a basketball. The ping-pong ball represents the atom nucleus, a small mass of positive charge. The nucleus is orbited by a number of electrons travelling at incredibly high speeds, which are particles of negative charge

nucleus without enough electrons. The electrons previous home can now also receive some other freed electrons also seeking a new home due to the created vacancy. The freed electrons know where to find a home because the net positive charge of the electron deficient nucleus attracts the negative charge of the roaming electrons. Thus, holes are created but are shortly filled again. (5)

A fundamental rule of physics states objects at rest tend to stay at rest unless moved by some outside force. All this moving required an initial push caused by the sunlight's energy. That energy got incorporated into the roaming electrons when they were ejected out of their orbits but it is once again released when the electrons once again find a home at a different nucleus with an electron shortage. This phenomenon is called the "Photovoltaic Affect". (5)

3.3. Types of Photovoltaic Cells

There are three basic categories of photovoltaic cells with several types in each category.

3.3.1. Crystalline Silicon Solar Cell

Flat plate collectors are most developed and prevalent types in use today. These include single crystal silicon and polycrystalline silicon, which is either grown or cost from molten silicon and later, sliced into cell size (see Figure 4). They are then assembled onto a flat plate surface, no lenses are used. As > 80% of solar cells produced at present are crystalline silicon solar cells (17) and remaining 20% are mostly amorphous silicon solar cells, almost all PV systems with > 1 kW peak power rating are fitted with crystalline silicon solar cells. These solar cells were until very recently exclusively based on the use of silicon wafers.

Wafer-based crystalline silicon solar cells have relatively high efficiencies, with commercial modules having efficiencies between 12 and 16 % and laboratory cells having efficiency of 24,4 %. These cells have already proven their excellent stability and reliability, operating under outdoor conditions without any deterioration in their

performance over several decades. The main disadvantage associated with this technology is the resulting high module price (27).

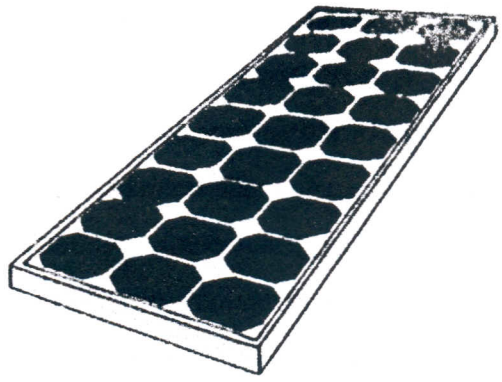

Figure 4: Crystalline silicon flat-plate module

3.3.1.1. Single-Crystal Silicon

In 1980, single-crystal silicon solar cells accounted for 90 percent of commercial photovoltaic cells. In 1990, they were only 35 percent of the total world market, with amorphous silicon at 31 percent and semicrystalline at 33 percent (16).

This process results in the waste of much silicon, as the cylindrical ingots are much larger in diameter than the required wafers. Alternative methods that minimise waste and cut manufacturing costs, such as the use of thinner saws to slice the wafers or direct growth of thin crystalline sheets or ribbons of silicon are being investigated actively to reduce manufacturing costs. These methods include a) the dendritic web approach, in which two dendrites a few centimetres apart are drawn from the melt, trapping a thin sheet of molten silicon in between, which solidifies b) the edge-defined film-fed (EFG) growth method, in which molten silicon moves by capillary action between two faces of a graphite die and a thin sheet is drawn from the top of the die and c) The S-Web approach, in which a carbon web is coated with silicon as it is drawn through a silicon melt (16).

One potential problem in photovoltaic manufacture is that the quantity of silicon that will be required in the near future, as the market of photovoltaic increases, is in excess of the current silicon waste produced by the semiconductor industry, indicating that silicon production specifically for the photovoltaic industry will be required. Silicon

is the second most abundant element on Earth, but it is present in the form of silica (silicon and oxygen) and silicates (compounds of silicon, oxygen, metals and possibly hydrogen). Silica is processed into silicon, which is then refined. The silicon used in photovoltaic manufacture can be less pure than that needed for semiconductors, but current production producers are expensive and some work is being carried out the develop new, low-cost methods for silicon production. (16)

Currently, efficiencies of experimental cells are 22 to 24 percent and those modules are 11 to 13 percent. Theoretical efficiencies for single-crystal silicon are 30 to 33 percent. A multi-junction device of a mechanically stacked gallium arsenide cell on top of single-crystal silicon cell is reported to have achieved 31 percent efficiency under concentrated light in 1988. (16)

3.3.1.2. Polycrystalline Silicon

A number of variables have to be controlled in preparing a polycrystalline film for a high performance cell. Some of them can be listed as; film thickness has to be optimised to account for the optical absorption depth and grain boundary recombination, grain size should be large (about 100 μm and 1 nm across) compared to the absorber layer thickness, the grain boundaries should show high resistance, epitoxy at the junction should reduce the recombination velocity at the interface and maximise the minority carrier diffusion length in that region. These requirements are quite demanding and the proper fabrication technique for polycrystalline silicon cells has been elusive. (24)

Polycrystalline cells are less efficient than single-crystal silicon cells, with efficiencies of 8 to 9 percent for field modules and 18 percent for experimental cells. However, the corresponding decrease in efficiency is compensated to a certain extent by the lower cost of manufacture for these cells. Silicon wafers are manufactured by cooling molten silicon in a crucible in a controlled manner to form an ingot, which is then cut into smaller blocks and sliced into wafers. Methods for producing thin films of silicon on different supports (such a ceramic and steel) are also being investigated, with the intention of reducing costs, as less is used in these devices. (16)

3.3.2. Thin-Film Solar Cells

Thin films required substantially less active material than single-crystal silicon.A typical thin film module is shown in Figure 5. Films are typically of thicknesses 0.001 to 0.002 mm, as opposed to about 0.3 mm for a typical thick-film single-crystal or polycrystalline silicon cell (8). Manufacturing techniques are also different, with thin layers of different materials being deposited sequentially, in a continuous process, on top of each other on a substrate (usually glass), from the back electrical contact (usually a thin layer of transparent oxide) to the semiconductor material to the antireflective coating to the front electrical contact, to eventually make up the module. The sheets are then divides into individual (interconnected) cells by scoring with a laser beam. The manufacturing procedures are potentially much less costly than growing single crystals, because in addition to using as little as 1 percent of active material compared with latter, they hold great potential for low-cost, automated, large scale production (16).

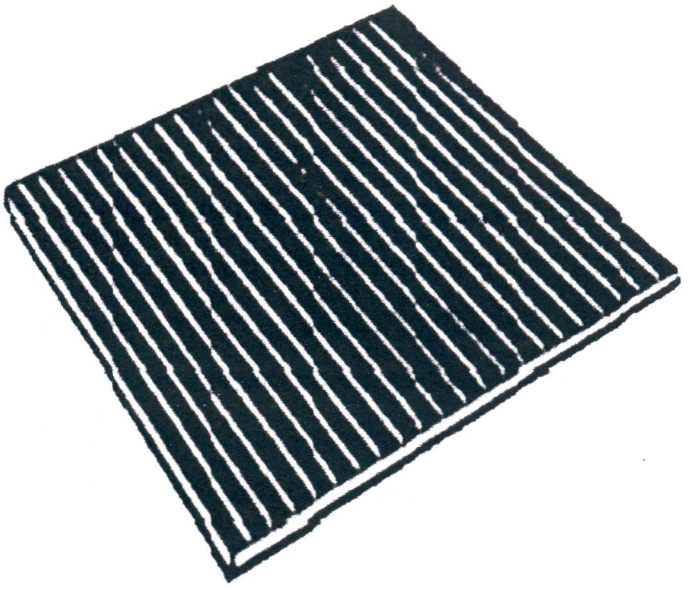

Figure 5: Thin film flat-plate module

3.3.2.1. Amorphous Silicon

Amorphous silicon (a glassy alloy of silicon and about 10 percent hydrogen) was regarded as an insukater until 1974, when it was demonstrated to be a semiconducting material. By 1990, amorphous silicon photovoltaic cells formed 31 to 32 percent of the world market for photovoltaic. The active cell has slightly different construction, with a neutral layer of amorphous silicon present between the thin, highly doped, top p-layer and the bottom n-layer. It is here that the electron-hole pairs are generated, thus facilitating their movement, as electrons and holes are far less mobile in amorphous silicon than crystalline silicon and doping worsens tis situation (16).

The cell had an initial efficiency of 1 percent in 1974, which decreased on exposure to light to as little as 0,25 to 0,5 percent (11). It is worth nothing that a decrease of 10 to 20 percent from the initial efficiency occurs in the first few months of use because of light-induced degradation of the amorphous silicon. Currently, stabilised monojunctional experimental cell efficiencies are about 6 percent and stabilised field module efficiencies are in the range of 3 to 5 percent. Estimates in the literature for theoretical efficiency limits for single-junction amorphous silicon cells are 22 percent and 27 to 28 percent. (16)

Multi-junctional devices, with higher efficiencies, have also been developed for amorphous silicon. Use of these configuration not only improves the overall efficiency of the cell bulk, in the case of amorphous silicon, results in a further increase in the overall efficiency of the individual cells because the thinner layers of material result in less light-induced degradation. The band gap of amorphous silicon can be altered by the formation of alloys with germanium, carbon, tin and nitrogen. Thus, typically three amorphous silicon cells with different band gaps are stacked to form a multi-junctional cell. Multi-junctional amorphous silicon cells have stabilised laboratory efficiencies of 10 percent. An amorphous silicon cell has also been stacked on top of a CIS (copper indium diselenide) cell, achieving initial efficiencies in the laboratory of 16 percent and 12 percent for submodel (16).

A major handicap of amorphous silicon solar cells and modules is their low efficiency values. The present laboratory record for stabilised efficiency is 13 % obtained on triple-junction cell. Actual commercial modules have stabilised efficiencies

between 4 and 8 % (20). The lower efficiency of the modules relative to single-crystal silicon is balanced by their significantly lower cost per unit area due to the smaller quantity of active material needed because of its high absorptivity (40 percent grater than single-crystal silicon), as well as the lower temperatures required for production and the use of low-cost substrates for depositing of the active material. (16)

To increase the efficiency of the amorphous silicon cell, a new type of cell structure has been introduced. The cell consists of three stacked cells, one of standard hydrogenated amorphous silicon while the other two cells use an alloy of silicon, germanium and hydrogen for the current generating layer. This amorphous silicon solar cell has already reached a conversion efficiency of 8,5 %. In laboratory conditions and is referred to as a stacked-junction or cascade cell. The higher efficiency results from capturing a larger percentage of solar radiation. Theoretical calculations of this three-cell structure with band gaps of 2, 1,7 and 1,45 eV give a conversion efficiency of 24 %. (8)

Advantages of amorphous silicon PV technology are the low deposition temperature (typically 200 ^{0}C), which permit the use of low-cost substrates, the possibility to easily integrate such modules into facades, roofs, and other structure, the option of implementing monolithically integrated electrical series connections within the solar cell structure itself (20).

3.3.2.2. Cadmium Telluride (CdTe)

The band gap energy, E= 1,45 eV, is very near the optimum value for single-junction solar cells. CdTe solar cells and modules are easier to fabricate than those from the CIS and CIGS system. A typical CdTe solar cell structure consists of an n-CdS and p-CdTe heterojunction deposited on a substrate coated with a TCO (28). Efficiencies of cadmium telluride-based laboratory photovoltaic cells are in the range of 12 to 16 percent, with prototype modules having efficiencies of 8 to 10 percent. Theoretical efficiencies are estimated at 27 to 28 percent. CdTe cells do not show the light-induced instability found in amorphous silicon. Two cell designs are predominant. In the first, CdTe forms the p-layer, and cadmium sulfide forms n-layer. However, CdTe highly resistive when doped, and this problem has been circumvented in another design that

makes CdTe into antrinsic layer, sandwiched between p-zinc telluride and n-cadmium sulfide. Cadmium telluride based cells are about to be commercialised, after benefiting from the experience to commercialise these cells (16).

An issue that has caused a considerable amount of debate is the toxicity of cadmium. On the hand CdTe is, as a compound, very stable and probably non-toxic. There are definite environmental hazards and safety issues related to the production of CdTe modules. The release of cadmium into the atmosphere in the case of fire, and the recycling of CdTe modules (28).

3.3.2.3. Copper Indium Diselenide (CIS):

Copper indium diselenide (CIS) and copper indium gallium diselenide (CIGS) are direct-gap polycrystalline semiconductors with very high optical absorption coefficients and are presently being widely studied for application in solar cells, with the corresponding module technology just reaching the stage of pilot production. CIS and CIGS are p-type semiconductors and are always used in a heterojunction structure, mostly with very thin n-type cadmium sulfide (CdS) layers (25).

Efficiencies of copper indium diselenide photovoltaic cells are in the range of 14 to 15 percent, with prototype modules demonstrating efficiencies of 11 percent. The theoretical efficiency for single-junction thin-film CIS cells is estimated as 23.5 percent by one source. These cells consist of a p-layer of cadmium sulfide. Copper indium diselenide is also both being used in various designs of multijunctional cells. An amorphous silicon solar cell has also been stacked on top of a CIS cell, achieving initial efficiencies in the laboratory of 16 percent (16).

CIS not only has high absorptivity, absorbing as much as 99 percent of the indecent light, but also displays good stability with regard to light degradation. CIS modules are amenable to low-cost, large-scale manufacture and are seen by many as the model thin film. It is worth nothing, however, that indium supply may become an issue if CIS modules enter large-scale production. Indium is thought to be as abundant is silver, but current supply capacity can not meet heavy feature demand. This could well lead to an increase in indium prices that would impede growth of CIS module

production. However, several companies have expressed interest in producing sufficient supplies of indium (16).

3.3.3. Concentrator Solar Cells

The high cost of the active semiconductor material has stimulated research into methods to reduce this cost further. One innovative idea is the concentrator cell. Here, mirrors or Fresnel lenses are used to concentrate the sunlight onto a smaller-area photovoltaic cell, allowing low-cost mirrors or lenses to replace high-cost photovoltaic cells. Furthermore, because only a small area of photovoltaic cell is required, one can pay a slightly higher price for it and still have lower overall cost compared with a conventional photovoltaic cell of the same material. Both single-crystal silicon and single-crystal gallium arsenide have been used in concentrator cells, as well as various multijunctional cells. Cell efficiency also appears to increase in concentrator cells, although the increase seems to depend on factors such as cell material and design. However, concentrator cells, unlike conventional cells, can not use diffuse sunlight and thus require direct-beam insolation, which is more variable than the total (diffuse plus direct) insolation at a particular site. (16) The view of typical concentrator solar cell is shown in Figure 6.

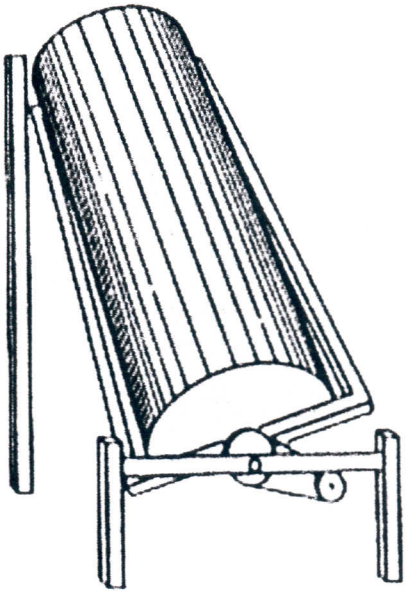

Figure 6: Concentrator PV module

3.3.3.1. Silicon

Several silicon photovoltaic concentrator systems have been installed and are operational. The efficiencies of laboratory concentrator cells are in the range 20 to 28 percent and of commercial concentrator modules under 20 suns are 15 to 17 percent.

3.3.3.2. Gallium Arsenide

Gallium arsenide is an excellent active material for use in photovoltaic cells because its band gap of 1,43 eV is near ideal for single-junction solar cells, it also has high absorptivity and it is relatively insensitive to heat. The last factor is particularly important in concentrator devices, where the cell is subjected to high temperatures. Single-crystal gallium arsenide, however, is very costly, and therefore its use in concentrator devices is more economical than its operation under regular light. To date, because its high cost, gallium arsenide has been primarily in modules for applications in space rather than for large-scale terrestrial uses. Approaches to reduce module costs include fabrication of cells on cheaper substrates, such as silicon or germanium.

Efficiencies for gallium arsenide cells under regular light are 20 to 25 percent; efficiencies for concentrator cells are in the range 28 to 30 percent. It is worth nothing that gallium arsenide devices show little difference between module and cell efficiency.

Much of current research on multijunctional cells focuses on gallium arsenide as either one or as all of the component cells. In 1988, the record for the highest efficiency (31 percent) photovoltaic device was set by gallium arsenide cell on top of a single-crystal silicon cell under concentrated light (16).

Chapter IV

CALCULATIONS

The performance of any solar thermal system depends on the solar radiation available to it. Solar radiation is characterised by its variability. Even when abundant, it varies during the day, reaching a maximum at noon when the path length through the atmosphere is the shortest. Unless the collector is continuously turned to face the sun, the sun's changing altitude and azimuth will reduce the collected heat below the potential maximum. The hours of daylight also vary seasonally, being the shortest in winter when the need for heat is the greatest. Therefore, unlike most other power production equipment, solar collectors remain dormant for one-third to two-third of the day, increasing system cost considerably (17).

Three types of solar radiation are useable by either active or passive terrestrial system. The most significant type of radiation for solar thermal process is called beam radiation or extraterrestrial radiation. Beam radiation is the solar radiation that travels from the sun to a point on the earth with negligible change in direction. It is the type of sunlight that casts a sharp shadow, and a sunny day it can be as much as 80 percent of the total sunlight strike the surface. In this study, this type of solar radiation will be calculated for solar charge station.

The second type of solar radiation is diffuse or scattered sunlight. This is sunlight that comes from all directions in the sky dome other than the direction of the sun. Scattering of sunlight produces it by atmospheric components such as particulate, water vapor, and aerosols. On a cloudy day the sunlight is 100 percent diffuse.

The third type of radiation that is sometimes present at the glazing of a solar collector or a window is reflected radiation. This is either diffuse or direct radiation reflected from the foreground onto the solar aperture. The amount of reflected radiation varies significantly with the nature of the foreground, being relatively higher for a light-coloured environment near the collector and relatively lower for a dark-coloured environment. The motion of the sun is important in determining the angle at which beam radiation strikes a surface. Therefore the first topic dealt with quantitatively has to do with the seasonal location of the sun relative to a viewer on the earth (15).

4.1. Extraterrestrial Solar Radiation

The total quantity of solar energy incident upon the earth is immense, but the energy is very diffuse and, because of the earth's rotation and orbit around the sun, cyclic both daily and seasonally. It also suffers from atmospheric interference from clouds, particulate matter, gases, etc. The energy incident on the earth outside of its atmosphere. This called extraterrestrial radiation.

The earth rotates around the sun on a slightly elliptical orbit with major and minor axes differing by 1,7 percent. The earth is closest to the sun on December 21 at a distance of about $1,45*10^{11}$ m, and farthest on June 22 at abut $1,54*10^{11}$ m, the average distance is $1,49*10^{11}$m (7).

The irradiance or intensity of the sun's radiant energy at the average earth-sun distance, measured normal to the earth-sun line but outside the earth's atmosphere, is called the solar constant, I_0^*. The value of I_0^* has been determined within an estimated accuracy of ± 1,5 % as 1353 W/m^2. This value has been derived from numerous measurements of direct solar radiation flux made through the atmosphere at a number of solar zenith angle, since the measured differences between them are directly translatable into a absolute measurement of the attenuation due to the atmosphere (17).

The extraterrestrial radiation from the sun is approximately the radiation of a black body at 5762 K, but shows certain peaks and valleys in the spectrum due to the radiative properties of the sun's incandescent gases. The black body and actual spectral irradiance are compared in Figure 7 (17).

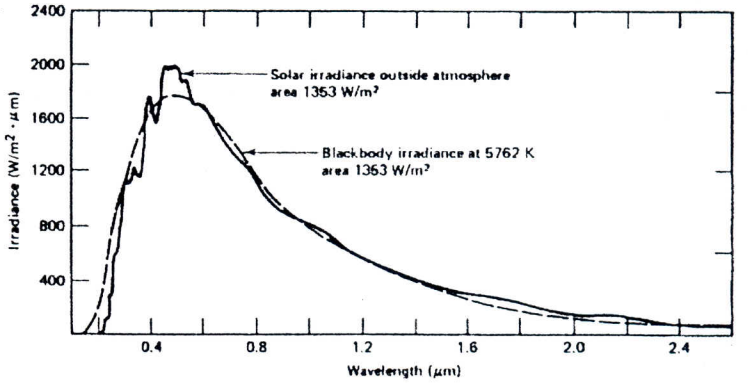

Figure 7: Solar spectral irradiance, standard curve, solar constant 1353 W/m^2

The apparent extraterrestrial solar irradiance I^*_{0n} vary over the year as the earth-sun distance changes seasonally, being about 3,5 % higher than I^*_0 in January and 3,5 % lower in June. These values can be closely approximated by the empirical formula:

$$I^*_{0n} = I^*_0 \ (1+ 0{,}033 \cos - \frac{360.n}{365}) \quad (W/m^2) \ (22) \qquad \text{(Equation 4.1)}$$

Where n is the number of the day in the year.

First of all, it must be known relation between local standard time and solar time for calculating solar radiation.

4.1.1. Equation of Time E

Solar time is based on the rotation of the earth about its polar axis and on its revolution around the sun. A solar day is the interval of time (not necessarily 24 h) as the sun appears to complete one cycle about a stationary observer on earth. The solar day varies in length through the year. The two principal factors for this variance are the following: (15) the earth sweeps out unequal areas on the ecliptic plane as it revolves around the sun, (3) the earth's axis is tilted with respect to the ecliptic plane. In simple terms, this means that if an observer facing the equator today sets a clock at 12 noon, clock time, the sun may not appear exactly over the local meridian. A discrepancy of as much as 16 min is possible (10). This discrepancy is called the equation of time and is measured relative to a perfectly uniform terrestrial motion. The following equation gives the equation of time:

$$E = 9{,}87.\sin(2B) - 7{,}5.\cos(B) - 1{,}5.\sin(B) \quad (min) \quad (22) \qquad \text{(Equation 4.2)}$$

Here B is;

$$B = \frac{360.(n-81)}{364}$$

Where n is the number of the day in the year, $1 < n < 365$. For less accurate calculations, the equation of time in minutes may be obtained from Figure 8:

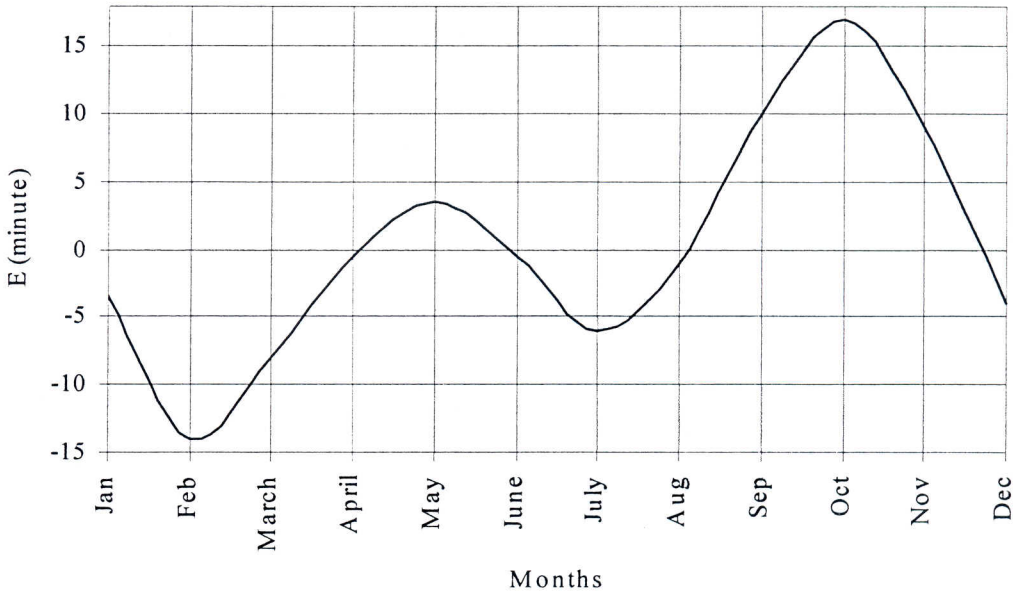

Figure 8:The Yearly Variation of the Equation of Time

Solar radiation data are often recorded in terms of local apparent time also called true solar time. On the other hand, some meteorological data such as temperature and wind speed are often recorded in terms of local clock time, which may be local standard time or daylight saving time. It is usually necessary to obtain the radiation, temperature, and wind velocity data for the same instant or duration. Therefore, it is desirable to convert local standard time to local apparent time. To carry out this conversion, it is necessary to know the standard meridian for the local time zone. All international standard meridians are multiples 15^0 east or west of Greenwich, England. Therefore, all standard times are hour multiples ahead of or behind the Greenwich Mean Time. (10).

Solar time for a given for a given local standard time can be written according to Duffie, Beckman and Whiller (2);

$$\text{Solar time} = \text{local standard time} \pm 4(L_{st} - L_{loc}) + E \qquad \text{(Equation 4.3)}$$

Where L_{st} is the standard longitude and L_{loc} is the local longitude. The longitude correction, 4 min for every degree, accounts for the difference between the local and standard meridians. It should be noted that the longitude correction is positive if the local meridian is east of the standard and is negative west of the standard meridian. The

value of the equation of time E is added algebraically, it may positive or negative. The correction for daylight saving time can be made appropriately (10).

4.1.2. Solar Incidence Angle

As known, solar beams reach the earth's surface two different ways, one of them is direct solar radiation, and other is diffuse solar radiation. To find the total extraterrestrial radiation, solar incidence angle must be calculated, the general angleθ between the normal to a surface of any orientation, anywhere on the earth, at any time, whether fixed or tracking and the incidence beam solar radiation is obtained (2):

$$\cos\theta = \sin\delta \cdot \sin\phi \cdot \cos\beta - \sin\delta \cdot \cos\phi \cdot \sin\beta \cdot \cos\gamma + \cos\delta \cdot \cos\phi \cdot \cos\beta \cdot \cos\omega + \cos\delta \cdot \sin\phi \cdot \sin\beta \cdot \cos\gamma \cdot \cos\omega + \cos\delta \cdot \sin\beta \cdot \sin\gamma \cdot \sin\omega \quad \text{(Equation 4.4)}$$

Here;

θ : Solar incidence angle.

δ : Declination angle.

β : Slope. It is the angle between the inclined surface and the horizontal plane

γ : Azimuth angle.

ω : Hour angle.

ϕ : Latitude. It is angular location north or south of the equator, north positive.

4.1.3. Solar Declination Angle, δ

The plane of revolution of the earth around the sun is called ecliptic plane. The earth itself rotates around an axis called polar axis, which is inclined at approximately $23{,}5^0$ from the normal to the ecliptic plane. The earth's rotation around its axis causes the diurnal changes in radiation income, the position of this axis relative to the sun causes seasonal changes in solar radiation. The angle between the polar axis and the normal to the ecliptic plane remains unchanged. The same is true of the angle between the earth's equatorial plane and the ecliptic plane. However, the angle between a line joining the centers of the sun and the earth to the equatorial plane changes every day, in

fact, every instant. This angle is called the solar declination δ. It is zero at the vernal and autumnal equinoxes and has a value of approximately $+23,5^0$ at the summer solstice and about -23.5^0 at the winter solstice. The four seasons pertain here to the Northern Hemisphere; the reverse is true in the Southern Hemisphere (10). It is illustrated in Figure 9.

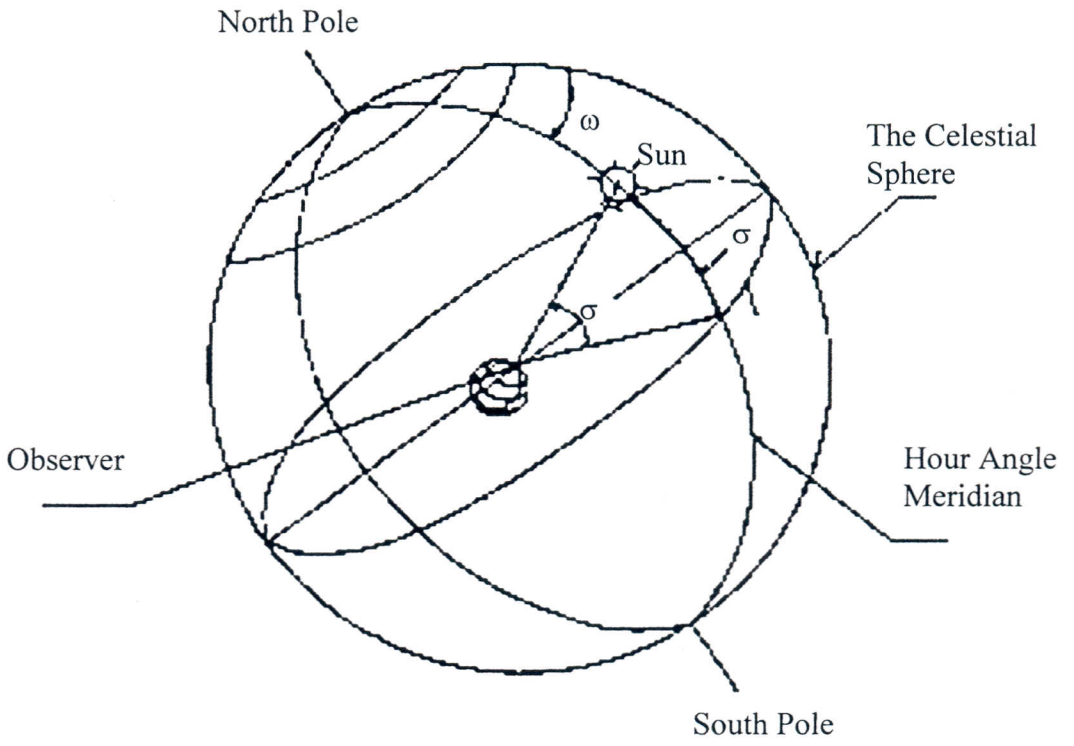

Figure 9: Declination and Hour Angles

Expressions giving the approximate values of solar declination with varying degrees of accuracy have been developed by a number of authors. Cooper presented the following expression for δ, in degrees:

$$\delta = 23,45 \,.\, \sin\left(360 \,.\, \frac{284 + n}{365}\right) \ (^0) \qquad \text{(Equation 4.5)}$$

Where n is the number of the day in the year.

4.1.4. Azimuth Angle, γ

The solar azimuth angle, measuring the relation of the sun to due south, depends on the same three angles as the solar altitude angle. The Figure 10 shows the solar altitude and azimuth angles. The Equation (4.6) can be used to calculate the solar azimuth angle:

$$\gamma = \sin^{-1}.\left(\frac{\cos\delta.\sin\omega}{\cos\phi}\right) \qquad \text{(Equation 4.6)}$$

The azimuth angle will be greater than 90^0 for some hours of the day when the length of day is greater than 12 h. Therefore, Equation (4.6) must also be evaluated relative to the time of year for which a calculation is being made. Near sunrise and sunset on days between March 21 and September 21 the azimuth angle will be greater than 90^0 (15).

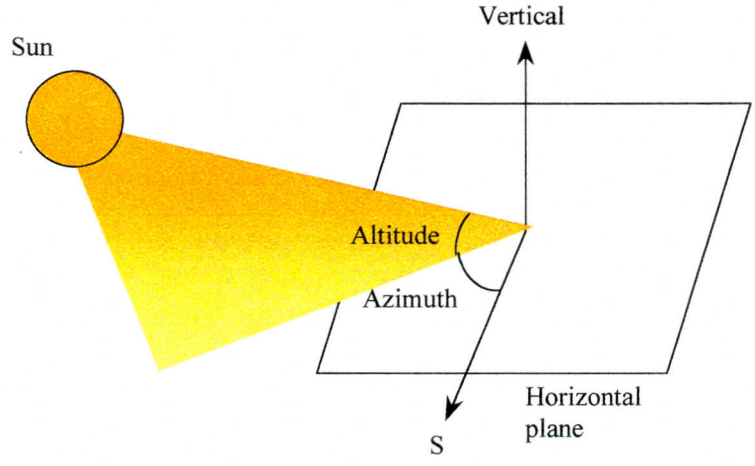

Figure 10: Azimuth and Altitude Angles

4.1.5. Hour Angle, ω

It is the angular displacement of the sun east or west of the local meridian due to rotation of the earth on its axis at 15^0 per hour. It takes morning negative and afternoon positive values. As the solar noon it is zero, ω = 0. All parameters are shown in Figure 11.

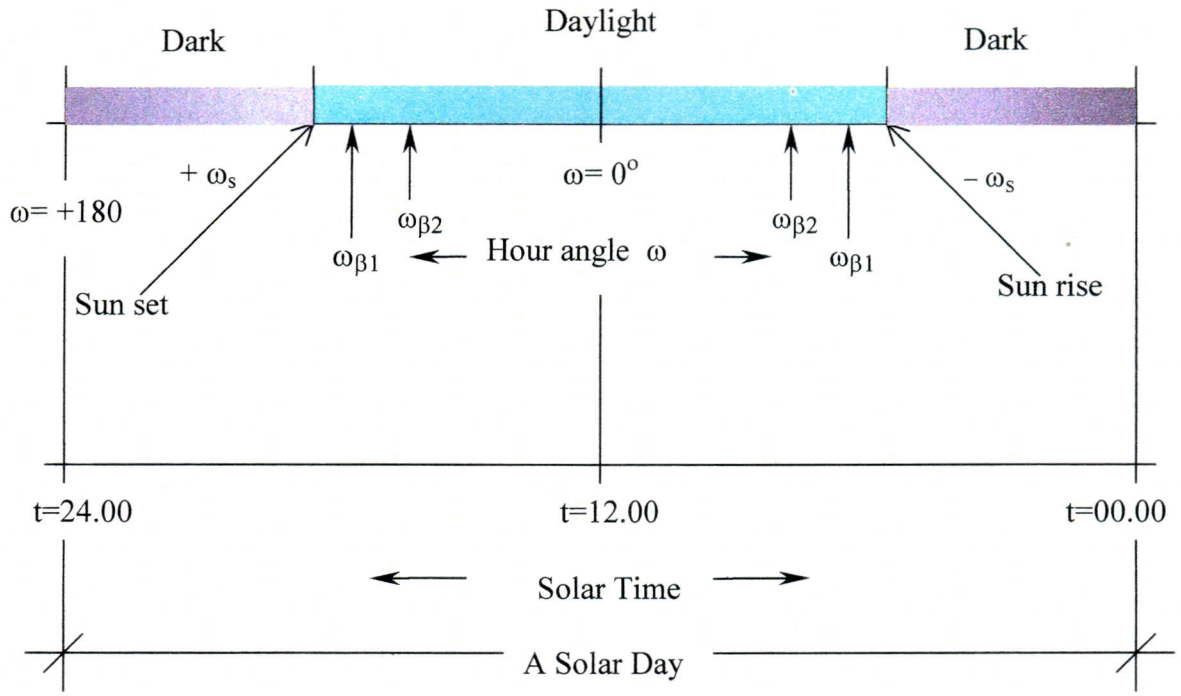

Figure 11:Sun-rise and Sunset on Horizontal and Inclined Surfaces

For an inclined surface, ω_β is defined as hour angle and $\omega_{\beta r}$ and $\omega_{\beta s}$ are defined as solar sunrise and sunset angles. The Equation (4.7) can be used for ω_β:

$$\omega_\beta = \arccos . \left(\frac{-N \mp \sqrt{N^2 - 4.M.P}}{2.M} \right) \qquad \text{(Equation 4.7)}$$

Here are:

$N = 2.K.L$; $M = L^2+E^2$; $P = K^2-E^2$; $K = A-B$; $L = C+D$

and

$A = \sin\delta . \sin\phi . \cos\beta$

$B = \sin\delta . \cos\phi . \sin\beta . \cos\gamma$

$C = \cos\delta . \cos\phi . \cos\beta$

$D = \cos\delta . \sin\phi . \sin\beta . \cos\gamma$

$E = \cos\delta . \sin\beta . \sin\gamma$

Two different roots are obtained from Equation (4.7):

$$\omega_{\beta 1} = \arccos . \left(\frac{-N - \sqrt{N^2 - 4.M.P}}{2.M} \right) \qquad \text{(Equation 4.8)}$$

$$\omega_{\beta 2} = \arccos . \left(\frac{-N + \sqrt{N^2 - 4.M.P}}{2.M} \right) \qquad \text{(Equation 4.9)}$$

The calculated values from Equation (4.8) and Equation (4.9), $\omega_{\beta 1}$ and $\omega_{\beta 2}$, are compared with horizontal plane sunrise, $-\omega$, and sunset, $+\omega$, angles. Then solar sunrise and solar sunset angles for inclined surface, $\omega_{\beta r}$ and $\omega_{\beta s}$, can be obtained (2).

If $\gamma = 0^0$;

$\omega_{\beta 1} = \omega_{\beta 2}$ and

$$\omega_{\beta 1} = \arccos . \left(\frac{-N}{2.M} \right) = \omega_{\beta 2} \quad \text{and} \qquad \text{(Equation 4.10)}$$

For solar sunrise;

$$\omega_{\beta r} = \text{Max} (-\omega_{\beta} , -\omega_s) \qquad \text{(Equation 4.11)}$$

and

For solar sunset;

$$\omega_{\beta s} = \text{Min} (\omega_{\beta} , \omega_s) \qquad \text{(Equation 4.12)}$$

If $-180^0 < \gamma < 0^0$

For solar sunrise;

$$\omega_{\beta r} = \text{Max} (-\text{Max} (\omega_{\beta 1}, \omega_{\beta 2}) , - \omega_s) \quad \text{and} \qquad \text{(Equation 4.13)}$$

For solar sunset;

$$\omega_{\beta s} = \text{Min} (\text{Min} (\omega_{\beta 1}, \omega_{\beta 2}) , \omega_s) \qquad \text{(Equation 4.14)}$$

If $0^o < \gamma < 180^0$

For solar sunrise;

$$\omega_{\beta r} = \text{Max} (-\text{Min} (\omega_{\beta 1}, \omega_{\beta 2}) , - \omega_s) \quad \text{and} \qquad \text{(Equation 4.15)}$$

For solar sunset;

$$\omega_{\beta s} = \text{Min} (\text{Max} (\omega_{\beta 1}, \omega_{\beta 2}) , \omega_s) \qquad \text{(Equation 4.16)}$$

If $\gamma = \mp \ 180^0$

$\omega_{\beta 1} = \omega_{\beta 2}$ and

For solar sunrise;

$$\omega_{\beta r} = \text{Max} (-\omega_{\beta} , -\omega_s) \quad \text{and} \qquad \text{(Equation 4.17)}$$

For solar sunrise;

$$\omega_{\beta s} = \text{Min}\,(\omega_{\beta}\,,\,\omega_{s}\,) \qquad \text{(Equation 4.18)}$$

4.2. Extraterrestrial Solar Radiation on Inclined Surfaces

The expressions for radiation on inclined surfaces will be formulated for different time periods; an hour, a day, a month and so forth.

4.2.1. Hourly Radiation

A surface tilted at an angle β toward the equator. Let $I_{oh\beta}$ be the extraterrestrial solar radiation on a surface tilted toward the equator (10). Then,

$$I_{oh\beta} = \frac{24.3600}{2\pi} \cdot \int_{\omega 1}^{\omega 2} I_0^{*} \,(1 + 0{,}033 \,.\, \cos \frac{360.n}{365}\,) \,.\, [\sin\delta \,.\, \sin\phi \,.\, \cos\beta - \sin\delta \,.$$
$$. \cos\phi. \;.\, \sin\beta \,.\, \cos\gamma + \cos\delta \,.\, \cos\phi \,.\, \cos\beta \,.\, \cos\omega + \cos\delta \,.\, \sin\phi \,.\, \sin\beta \,.$$
$$. \cos\gamma \,.\, \cos\omega + \cos\delta \,.\, \sin\beta \,.\, \sin\gamma \,.\, \sin\omega\,].\, d\omega \qquad \text{(Equation 4.19)}$$

The integration of Equation (4.19) between the sunrise and sunset hour angle results in an expression for the hourly solar radiation $I_{oh\beta}$. Consequently,

$$I_{oh\beta} = \frac{24.3600}{2\pi} \,.\, I_0^{*}(1 + 0{,}033 \,.\, \cos \frac{360.n}{365}) \,.\, [\sin\delta \,.\, \sin\phi \,.\, \cos\beta \,.\, \frac{2\pi}{360}\,(\omega_2 - \omega_1) -$$
$$- \sin\delta \,.\, \cos\phi. \;.\, \sin\beta \,.\, \cos\gamma \,.\, \frac{2\pi}{360}\,(\omega_2 - \omega_1) + \cos\delta \,.\, \cos\phi \,.\, \cos\beta \,.\, (\sin\omega_2 -$$
$$- \sin\omega_1) + \cos\delta \,.\, \sin\phi \,.\, \sin\beta \,.\, \cos\gamma \;(\sin\omega_2 - \sin\omega_1) - \cos\delta \,.\, \sin\beta \,.\, \sin\gamma \,.$$
$$. (\cos\omega_2 - \cos\omega_1)\,] \;\; (J/m^2) \qquad \text{(Equation 4.20)}$$

4.2.2. Daily Radiation

The daily extraterrestrial solar radiation on a inclined surface can be calculated Equation (4.21):

$$I_{on\beta} = \frac{24.3600}{2\pi} \int_{\omega\beta,r}^{\omega\beta,s} I^{*}_{on} \; . \; \text{Cos}\,\theta \; . \; d\omega \qquad \text{(Equation 4.21)}$$

The integration of Equation (4.21), daily extraterrestrial solar radiation expression can be obtained.

$$I_{on\beta} = \frac{24.3600}{2\pi} I^{*}_{0}.(1 + 0{,}033 \; . \; \cos \frac{360 \; .n}{365}) \; .[\; \sin\delta \; . \; \sin\phi \; . \; \cos\beta \; . \; \frac{2\pi}{360}(\omega_{\beta s} - \omega_{\beta r}) -$$

$$- \sin\delta \; . \; \cos\phi \; . \; \sin\beta \; . \; \cos\gamma \; \frac{2\pi}{360}(\omega_{\beta s} - \omega_{\beta r}) + \cos\delta \; . \; \cos\phi \; . \; \cos\beta \; . \; (\sin\omega_{\beta s} -$$

$$- \sin\omega_{\beta r}) + \cos\delta \; . \; \sin\phi \; . \; \sin\beta \; . \; \cos\gamma \; (\sin\omega_{\beta s} - \sin\omega_{\beta r}) - \cos\delta \; . \; \sin\beta \; . \; \sin\gamma .$$

$$. \; (\cos\omega_{\beta s} - \cos\omega_{\beta r}) \quad (J/m^2) \qquad \text{(Equation 4.22)}$$

Chapter V

EXPERIMENTAL WORK

The second part of this study was installation of modules on the roof and measurements of the solar insolation. The current intensities and the voltage of the system were measured by means of voltameter and ampere-meter. After these measurements solar powers have been calculated hourly for a day where experiments have been carried out. According to these total solar powers were obtained as daily average values. These values have been compared the with measured data by Solar Energy Institute of Aegean University and data given by Meteorological Station in Güzelyalı – Izmir.

5.1. Experimental Set-Up

Omega type solar charge station was located at the Electrical Engineering Department's roof in Gülbahçe, in Izmir. This solar charge station has 16 photovoltaic modules, which are composed of crystalline silicon solar cell. The modules were mounted on aluminium. The bearing constructions are connected to each other as parallel in order to increase the electrical current intensities. After connections of photovoltaic, three headlights of a car were used as load and three ampere-meters were connected to the lambs for measuring of the current intensity, I (ampere), (see Figure 12 (A)). Because of the total current intensities have very high values, the three lamb were connected to the system to decrease the intensity for each lamb. As a result of this, the total current intensities were divided in to the three parts. Thus, the summation of these three current intensity values gives the total current intensity. For all calculations of power, these hourly total current intensity values were taken. Before connecting three head light of a car to the system, the voltage, V (volt), is measured as 20 V (see Figure 12 (B)). This value is constant for parallel connection and it is taken as 20 Vin all experiments. After preparing the experimental set-up, current intensities were measured hourly. After finding current intensities and voltage of the omega type solar charge

station, the powers, P (W), of the system were calculated hourly. But at sunset and sunrise times the current of the electricity could not be measured.

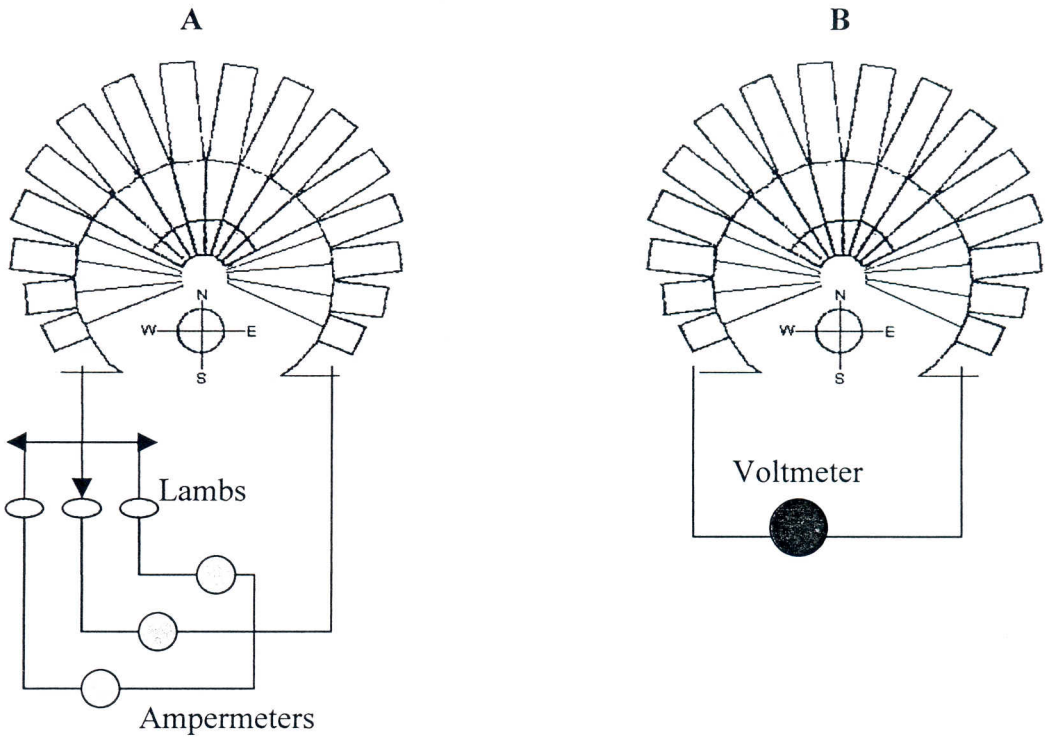

Figure 12: Experimental set-up for measurement of Current Intensity (A), and measurement of Voltage (B), schematically

5.2. Experiments

Measurements have been carried out from 28 June 2000 to 15 October 2000. But, only the data of the experiments, which are done on 28 September and 15 October 2000, have been given in this thesis.

First of all, on 28 September and on 15 October current intensities were measured from 09:00 to 17:00. But the sunrise and sunset times the current intensities have not been measured. For each time period, for example 09:00-10:00, three different current intensity values and the voltage were read with ampere-meters and voltmeters. The summation of these three taking different current intensities, the power could be calculated as follows:

$P = I * V$ (W) (Equation 5.1)

On 28 September 2000, the current intensity values, powers and voltage are shown in Table 5.2.1:

Table 5.2.1. Experimental data on 28 September 2000 for Omega Type Charge Station

Time Interval (h)	Current Intensity (A)	Voltage (V)	Power (W)
09:00 – 10:00	14,300	20	286
10:00 – 11:00	17,200	20	344
11:00 – 12:00	20,020	20	400
12:00 – 13:00	20,300	20	406
13:00 – 14:00	20,100	20	402
14:00 – 15:00	20,500	20	410
15:00 – 16:00	20,120	20	402,4
16:00 – 17:00	18,400	20	368
17:00 – 18:00	11,300	20	226

On 15 October 2000, the current intensity values, powers and voltage are shown in Table 5.2.2:

Table 5.2.2. Experimental data on 15 October 2000, for Omega Type Charge Station

Time Interval (h)	Current Intensity (A)	Voltage (V)	Power (W)
09:00 – 10:00	14,560	20	291,2
10:00 – 11:00	18,650	20	373
11:00 – 12:00	21,000	20	420
12:00 – 13:00	22,490	20	449,8
13:00 – 14:00	24,060	20	481,2
14:00 – 15:00	25,660	20	513,2
15:00 – 16:00	22,220	20	444,4
16:00 – 17:00	18,5400	20	370,8
17:00 – 18:00	-	20	-

After determining of solar power obtained, they were compared with the calculated values and measured data by Solar Energy Institute of Ege University and meteorological station in Güzelyalı. Data were taken from meteorological station in Güzelyalı and Solar Energy Institute of Ege University and obtained power are given in Table 5.2.3:

Table 5.2.3. Obtained Solar Power from Experiment, Measured Values of Direct Solar Radiations at the Meteorological Station in Güzelyalı, Measured Data at Solar Energy Institute, on 28 September 2000

Time Interval (h)	Obtained Power (experimental), MJ	Meteorological Station Data , MJ	Solar Energy Institute Data (MJ)
09:00 – 10:00	1,0296	10,8175	-
10:00 – 11:00	1,2384	12,7929	-
11:00 – 12:00	1,4414	11,7956	-
12:00 – 13:00	1,4616	11,7037	-
13:00 – 14:00	1,4472	12,6721	-
14:00 – 15:00	1,4760	6,4086	-
15:00 – 16:00	1,4486	2,7965	-
16:00 – 17:00	1,3248	3,7375	-
17:00 – 18:00	0,8136	3,8977	-

On 28 September 2000, there was no any measured value at Solar Energy Institute. In the Table 5.2.3, data from the meteorological station are direct solar radiations on inclined surfaces. Photovoltaic modules use only direct beam radiations, not values of total radiations

On 15 October 2000 after measured current intensities for each time period obtained power values are calculated from P = I *V and direct solar radiations data from the meteorological station and measured values of Solar Energy Institute are given in Table 5.2.4:

Table 5.2.4. . Obtained Solar Power from Experiment, Measured Values of Direct Solar Radiations at the Meteorological Station in Güzelyalı, the Measured data at Solar Energy Institute, on 15 October 2000

Time Interval (h)	Obtained Power (experimental), MJ	Meteorological Station Data , MJ	Solar Energy Institute Data (MJ)
09:00 – 10:00	1,04383	11,5534	5,3955
10:00 – 11:00	1,3428	12,8792	8,5638
11:00 – 12:00	1,5120	13,0739	4,8761
12:00 – 13:00	1,6192	13,0731	10,4529
13:00 – 14:00	1,7323	12,7466	7,6106
14:00 – 15:00	1,8475	11,4661	7,4758
15:00 – 16:00	1,5998	6,2948	4,2390
16:00 – 17:00	1,3349	5,6646	2,3758
17:00 – 18:00	-	-	

In the Table 5.2.4, all meteorological data are direct solar radiation on inclined surfaces, not values of total solar radiations.

The values in Table 5.2.3 and Table 5.2.4 will be used in section 5.5 in order to calculate the efficiency coefficients of the omega type solar charge station.

5.3. Calculation of Direct Solar Radiation on a Horizontal Surface

Data from the meteorological station in Güzelyalı are values of the total solar radiations on horizontal surface. But our solar charge station has 16 inclined surfaces, so data of meteorological station on a horizontal surface were calculated again for inclined surfaces for each time period which slopes were taken as same as omega type solar charge station. Unfortunately, the rays falling on a surface are partly direct and partly diffuse. These meteorological data represent total solar radiation on a horizontal surface and these values are summation of direct and diffuse solar radiations. But, photovoltaic modules can not use diffuse sunlight and thus require direct beam insolation. The

meteorological data are shown in Figure 16 and Figure 17 as total solar radiation on horizontal surfaces.

The direct solar radiation on a horizontal surface, I_{ihz}, is equal to difference between total radiation which is taken from meteorological station, I_{thz}, and diffuse radiation, I_{dhz}, on a horizontal surface;

$$I_{ihz} = I_{thz} - I_{dhz} \qquad \text{(Equation 5.2)}$$

First of all, diffuse solar radiation on a horizontal surface must be found for calculating direct solar radiation on a horizontal surface. According to Duffie and Beckman (2), there are some relations between diffuse solar radiation and total solar radiation at one hour:

$$I_{dhz} / I_{thz} = 1{,}00 - 0{,}1.\ (I_{thz} / I_{ctz}) \qquad \text{(Equation 5.3)}$$

For $0 \leq I_{thz} / I_{ctz} < 0{,}48$

$$I_{dhz} / I_{thz} = 1{,}11 + 0{,}039.\ (I_{thz} / I_{ctz}) - 0{,}789.\ (I_{thz} / I_{ctz}) \qquad \text{(Equation 5.4)}$$

For $0{,}48 \leq I_{thz} / I_{ctz} < 1{,}11$

$$I_{dhz} / I_{thz} = 0{,}2 \quad \text{for} \quad I_{thz} / I_{ctz} \geq 1{,}11 \qquad \text{(Equation 5.5)}$$

In these equations, I_{ctz} is total solar radiation on a clear day on a horizontal surface that is equal to summation of direct solar radiation, $I_{cız}$, and diffuse solar radiation, I_{cdz}, on a clear day and on a horizontal surface:

$$I_{ctz} = I_{cız} + I_{cdz} \qquad (J/m^2) \qquad \text{(Equation 5.6)}$$

And,

$$I_{cız} = I^{*}_{cı}.\ 3600 \qquad (J/m^2) \qquad \text{(Equation 5.7)}$$

$I_{cdz} = I^{*}_{cdz} \cdot 3600$ (J/m^2) (Equation 5.8)

In these equations, $I^{*}_{cı}$ is direct solar radiation and I^{*}_{cdz} is diffuse solar radiation on a clear day and on a horizontal surface:

$$I^{*}_{cı} = I^{*}_{on} \cdot \tau_1 \cdot \cos\theta_z \quad (W/m^2) \qquad \text{(Equation 5.9)}$$

$$I^{*}_{cdz} = I^{*}_{on} \cdot \tau_d \cdot \cos\theta_z \quad (W/m^2) \qquad \text{(Equation 5.10)}$$

τ_1 and τ_d are permeability factors for direct and diffuse solar radiations on a clear day. They can be calculated from following equations:

$$\tau_1 = a_0 + a_1 \cdot e^{-(k / \cos\theta_z)} \qquad \text{(Equation 5.11)}$$

$$\tau_d = 0{,}2710 - 0{,}2939 \cdot \tau_1 \qquad \text{(Equation 5.12)}$$

a_0 , a_1 and k are calculated with helping of a^{*}_0, a^{*}_1 and k^{*} :

$$a^{*}_0 = 0{,}4237 - 0{,}00821 \cdot (6 - A^2) \qquad \text{(Equation 5.13)}$$

$$a^{*}_1 = 0{,}5055 + 0{,}00595 \cdot (6{,}5 - A^2) \qquad \text{(Equation 5.14)}$$

$$k^{*} = 0{,}2711 + 0{,}001858 \cdot (2{,}5 - A^2) \qquad \text{(Equation 5.15)}$$

A is a location of observer as km.

$r_0 = a_0 / a^{*}_0$; $r_1 = a_1 / a^{*}_1$; $r_k = k / k^{*}$ are constants for middle-parallel in summer and values of them 0,97, 0,99, 1,02 are respectively.

θ_z, in Equations (5.8) and (5.9), is zenith angle. It can be calculated from:

$$\cos\theta_z = \sin\phi \cdot \sin\delta + \cos\phi \cdot \cos\delta \cdot \cos\omega \qquad \text{(Equation 5.16)}$$

ϕ, δ and ω were explained in Chapter IV.

I^{*}_{on} is intensity of extraterrestrial solar radiation Its empirical formula was given in Equation (4.1), in Chapter IV. After finding all required values, we can calculate I_{ihz} for each hour, easily.

5.4.Calculation of Direct Solar Radiation on Inclined Surface

The direct beam radiation falling on an inclined surface using the intensity on a horizontal surface and the radiation for direct beam, ratio factor R_I:

$$I_{th\beta} = I_{ihz} . R_I \qquad \text{(Equation 5.17)}$$

Where

$$R_I = \text{Cos}\ \theta\ /\ \text{Cos}\ \theta_z \qquad \text{(Equation 5.18)}$$

Cos θ was defined in Chapter IV. That's why in this chapter we do not give again. After having Cos θ and Cos θ_z , calculate the direct beam radiation falling onto an inclined surface. All calculated values are given in Table 5.4 .1 and Table 5.4.2.

5.5. Calculation of Efficiency of the Photovoltaic Modules

The amount of the total energy is 11,6812 MJ on 28 September and 12,0368 MJ on 15 October. The total amount of the energy on 28 September 2000 calculated from the meteorological data given by Meteorological Station in Güzelyalı is 78,6164 MJ and on 15 October is 86,7517 MJ According to our measurements. The definition of the efficiency of omega type solar charge station is given below:

$$\text{Efficiency of the station} = \frac{\text{calculated solar energy daily collected by solar charge station}}{\text{solar radiation daily average direct beam}}$$

According to readings on 28 September 2000, Figure 18:

$\text{Efficiency}_1 = 11,6812 / 78,6164 = 0,13$

The readings on 15 October 2000, Figure 19:

$$Efficiency_2 = 12,0368 / 86,7517 = 0,13$$

And the readings on 15 October, Figure 20:

$$Efficiency_3 = \frac{\text{calculated solar energy daily collected by solar charge station}}{\text{solar radiation values by solar energy institute}}$$

$$Efficiency_3 = 12,0368 / 50,9895 = 0,24$$

5.6.Evaluation of Experimental Results

According to the literature, efficiency of silicon photovoltaic cells is between 11% to 13%. When our omega type solar charge station is compared with amount of the direct solar energy values from meteorological station in Güzelyalı on 28 September and on 15 October (see Figure 18–19), efficiency of our system is 13%. This value is the same in the literature. The results of the experiments, the total amount of the solar energy are 11,6812 MJ on 28 September and 12,0368 MJ on 15 October. According to meteorological station data the total amount of energy on 28 September is 78,6164 MJ and on 15 October is 86,7517 MJ.

The third efficiency which was calculated according to the experimental values and values of Solar Energy Institute, was found 24% only on 15 October. The total amount of measured daily radiation from Solar Energy Institute of Ege University is 50,9895 MJ (see Figure 20) On 15 October, 12,0368 MJ energy could be obtained by omega type solar charge station.

For finding more accurate values of efficiency, the amounts of the energies must be compared hourly. And the location of the Meteorological Station, Solar Energy Institute and our experimental set-up are very different. Thus, obtained energies and the efficiencies have different values.

It is obvious from Figure 18, Figure 19 and Figure 20, efficiency coefficients differs from each other. But, Figure 20 gives very high efficiency for the system. On the

other hand, the meteorological data have a little bit less accuracy for solar insolation. Because of the accuracy of the solarimeter. Offcourse and readings may have also some subjective in accuracy but the reading of voltage and current intensity does not involve to much instrumental in accuracy. But in Laboratories of Frauenhofer Gesellschaft in Freiburg – Germany, they claim that photovoltaic cells can give up to 27% efficiencies.

Chapter VI

ECONOMIC AND ENVIRONMENTAL ANALYSIS

6.1. Economics of Photovoltaic Cells

Photovoltaic cells produce electricity when sunlight excites electrons in the cells Photovoltaic cells are ideal for use in homes, industries and utilities. Because of the size of the units is flexible and adaptable, (19). The main obstacle that prevents the widespread use of photovoltaic is cost. In some applications, such as in remote areas, photovoltaics are already cost effective, if photovoltaic must complete with fossil technologies for the extensive grid market, significant reduction in cost are required (18).

Currently, production of electricity from photovoltaic cells costs approximately 30 cents/kWh (23), but the price is projected to fall to approximately 10 cents/kWh by the end of the decade and perhaps reach as low as 4 cents by the year 2030, provided the needed improvements are made. In order to make photovoltaic cells truly competitive, the target cost for modules would have to be approximately 8 cents/kWh. Using photovoltaic modules with an assumed 7,3% efficiency, 1 billion kWh/year of electricity could be produced on approximately 2700 ha of land, or approximately 0,027 ha per person, based on the present average per capita use of electricity. If 21% efficient cells were used, the total area needed would be greatly reduced. Photovoltaic plants with this level of efficiency are being developed. The energy input for the structural materials of a photovoltaic system delivering 1 billion kWh is calculated to be approximately 300 kWh/m^2. The energy input/output ratio for production is about 1:9 assuming a life of 20 years. Locating the photovoltaic cells on the roofs of homes, industries and other buildings would reduce the need for additional land by approximately 5%, as well as reduce the costs of energy transmission. However, photovoltaic systems require back-up with conventional electrical system, because they function only during daylight hours (23).

The main challenge now is to reduce manufacturing cost to the point where photovoltaic can compete economically in a sequence of increasingly big market

segments. The photovoltaic market has undergone a sharp upsurge that has persisted since about 1980. In 1997 alone, the market grew by more than 40% (4). Markets and technologies total shipments of photovoltaic modules hit 124,3 MW in 1997. The growth rate for these shipments is predicted to increase at an average annual growth rate of 22,3% reaching 421,3 MW by 2003 (12).

6.2. Environmental Issues

The total amount of primary energy, which is consumed in the production of frameless thin film modules, the gross energy requirement, has been estimated to be 1100–1900 MW/m^2, of module area for present-day production technologies. This gross energy requirement value includes the energy required for cell processing, for the production of input materials, for the production of capital equipment and the indirect process energy (heating, lighting, emission control).

The higher gross energy requirement value in the range represents amorphous silicon and CIS modules, while the lower value is found for CdTe modules manufactured by means of electrodeposition. Future improvements in production technology are expected to reduce the gross energy requirement values to below 1100 MJ/m^2.

Calculation of the energy pay-back time assuming a module efficiency of 5% respectively 10%, an irradiation of 1700 kWh/m^2/year, a system performance ratio of 0,80 (grid connected system) and a thermal to electric conversion of 0,4 results in a value 1,8–3 years for present-day technology and below one year for future technology.

Although the use of cadmium or selenium compounds in solar cell modules may give rise to public concerns the risks of this should not be exaggerated. Considering CdTe and CIS layer thickness of a few μm the cadmium or selenium content of thin film modules is comparable or much lower than that of accepted products like NiCad penlight batteries. On the other hand, one should note that CdTe modules with much thicker layers are also available on the market today and also that environmental regulation with regard to cadmium will be increasingly strict. As regard module manufacturing conditions and if standard emission control measures are implemented

no serious emissions to the environment are expected from the production of all three modules type.

However, for deposition process with a low material efficiency and a high material consumption, like spraying or screen printing, it will be more difficult to achieve a low emission rate, than for a process like electrodeposition which has a high material efficiency and which takes place in an aqueous environment.

External safety risks from module manufacturing are mainly due to the storage and handling of explosive and toxic gases. The storage of large quantities of silane for a-I production and of hydrogen selenide for CIS production may pose serious safety risks for workers and public. For CIS the use of deposition methods which do not rely on the selenization process are therefore highly preferable.

Health risks resulting form the use of CdTe and CIS modules have been evaluated for a number of different exposure routes (eg emissions during a fire, emissions from broken modules). In all these cases the risks were found to be negligible or small.

A life-cycle comparison of emission on the basis of generated electricity shows that the estimated Cd or Se emissions from CdTe or CIS modules are comparable or lower than the cadmium or selenium emissions from coal-fired generation of electricity. It should be noted, however, that a coal plant has several more, environmentally harmful emissions.

The emissions from CdTe and CIS module include the releases from Cd/Se winning, module manufacturing, fires in rooftop photovoltaic installations and from incinerator of 10% of the module waste (1)

6.3. Comparing Solar Power to Coal and Nuclear Power

Coal and nuclear power production are included in this analysis to compare conventional source of electricity generation to various future solar energy technologies. Coal, oil, gas, nuclear and other mined fuels are used to meet 92% of world energy needs. Energy efficiencies for both coal and nuclear fuels are low due to the thermal law constraint of electric generator designs. Coal is approximately 35% efficient and nuclear fuels approximately 33%. Both coal and nuclear power plants in the future may require

additional structural materials to meet clean air and safety standards. However, the energetic requirements of such modifications are estimated to be small compared with the energy lost due to conversion inefficiencies. The costs of producing electricity using coal and nuclear energy are 3 cents and 5 cents per kWh, respectively. However, the costs of this kind of energy generation are artificially low because they do not include such external costs as damages from acid rain produced from coal and decommissioning costs for the closing of nuclear plants. The clean air act and its amendments may raise coal generation costs, while the new reactor designs, standardisation and streamlined regulations may reduce nuclear generation costs.

The mined-energy-industry, like the gasoline industry, does not pay for the environmental and public health costs of fossil energy production and consumption.

The land requirements for fossil fuel and nuclear plants are lower than those for solar energy technologies. The land area required for electrical production of 1 billion kWh/year is estimated at 363 ha for coal and 48 ha for nuclear fuels. These figures include the area for the plants and both surface and underground mining operations and waste disposal. The land requirements for coal technology are low because it uses concentrated fuel sources rather than diffuse solar energy. However, as the quality of fuel ore declines, land requirements for mining will increase. In contrast, efficient reprocessing and the use of nuclear breeder reactor may decrease the land area necessary for nuclear power. Many environmental problems are associated with both coal and nuclear power generation. For coal, the problems include substantial damage to land by mining, air pollution, acid rain, global warming, as well as the safe disposal of large quantities of ash. For nuclear power, the environmental hazards consists mainly of radioactive waste that may last for thousands of years, accidents and the decommissioning of old nuclear plants. Fossil fuel electric utilities account for tw0-thirds of the sulfur dioxide, one-third of the nitrogen dioxide and one-third of the carbon dioxide emissions. Removal of carbon dioxide from coal plant emissions could raise cost to 10 cents/kWh, a disposal tax on carbon could raise coal electricity costs to 18 cents/kWh. The occupational and public health risks of both coal and nuclear plants are fairly high, due mainly to the hazards of mining, ore transportation and subsequent air pollution during the production of electricity. However, there are 22 times as many deaths per unit of energy related to coal than of nuclear energy production because

90000 times greater volume of coal than of nuclear ore is needed to generate an equivalent amount of electricity. Also and as important coal produces more diffuse pollutant than nuclear fuels during normal operation of the generating plant. Coal fired plants produce air pollutants, which are including sulfur oxides, nitrogen oxides, carbon dioxide, and particulate, that adversely affects air quality and contributes to acid rain. Technologies do exist for removing most of the air pollutants, but their use increases the cost of a new plant by 20-25%. (23).

Chapter VII

RESULTS AND DISCUSSION

In this thesis, for charging the battery of an electric car, five different type of solar charge station was researched which could be placed on garage roofs and has 16 vertical photovoltaic cells. These called are photovoltaic charge stations or solar charge stations. These are omega type solar charge station (first combination), south facing charge station with different angles (second combination), south facing solar charge station with fixed angles (third combination), inverse of omega type solar charge station (fourth combination), and optimisation of south facing solar charge station (fifth combination). Calculations of solar radiation were described in detail in Chapter IV.

7.1. Omega Type Solar Charge Station (First Combination)

In the first combination, 16 photovoltaic modules were installed like an omega, Ω. First of all, slope combinations will be obtained with calculating of extraterrestrial solar radiation, after they are compared with measured values. The corresponding values are given in Table 7.1. In the table, γ are azimuth angles in degrees, β are slope of the photovoltaic modules in degrees, H is heights in meter and L are projected length of modules in meter. After trying many angles of azimuth and slopes of the modules, the following angles for the 16 modules, 1 to 8 of them on the East Side and 9 to 16 on the West Side have been chosen from Atagündüz (2).

After having the incidence angles one can calculate the extraterrestrial solar energy falling into the all-photovoltaic modules. After calculating solar radiation first combination is compared with other types of photovoltaic charge stations. According to the Table 7.1, maximum energy that is 556,579 MJ/m^2 in June, and minimum energy that is 316,4446 in December were calculated for omega type solar charge station. But amount of the solar energy of the reflected beams could not be calculated and shades of the photovoltaic were not discussed. For the extra solar energy gain, the vertical reflectors must be integrated to the system.

The optimum slopes of modules and the maximum amount of solar radiation are given in Table 7.5.2. The calculated values of these are illustrated in Figures 21-36. The omega type solar charge station has mainly advantages against the other types of photovoltaic solar charge stations. The required area for construction is small, 3,5 m^2. Therefore it is easy to installation the roof of garages. If the vertical reflectors are integrated to the system, these give additional solar energy gain. Therefore, fluctuation of the total energy curve over one year period is the less than the system of without reflectors. The omega type solar charge station is shown in Figure 13.

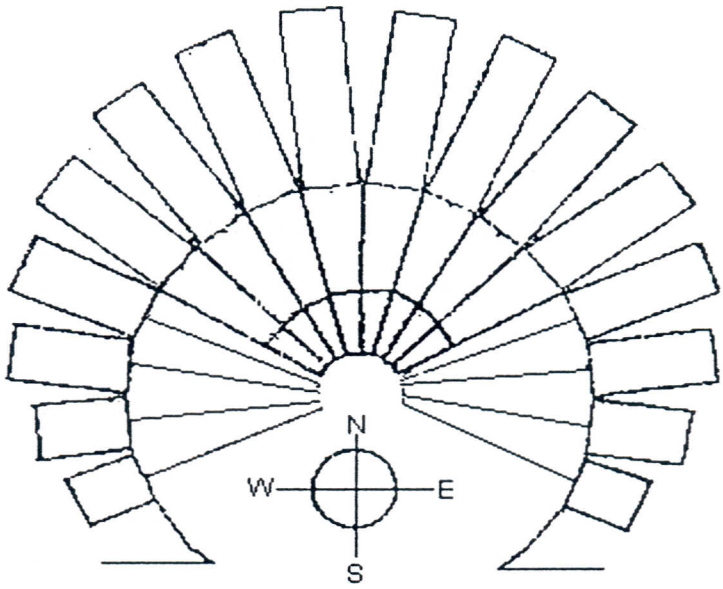

Figure 13: Omega Type solar charge station, schematically

7.2. South Facing Solar Charge Station with Different Angles (Second Type)

In second type of solar charge station, faces of the whole modules are turned to the south side. But the slopes of the modules are same in the first combination. That's why azimuth angles are equal to zero in second type solar charge station. Extraterrestrial solar radiation value, slopes of modules and azimuth angles are given in Table 7.2. These energy values were calculated as monthly average daily extraterrestrial solar radiation. In second type solar charge station, maximum energy is 565,6868 MJ/m^2 in March and minimum energy is 479,1024 MJ/m^2 in December. In Figure 37, first type

and second type solar charge stations were compared. According to the data second type solar charge station can be collected more energy than the first type solar charge station. The fluctuation of the total energy in second type solar charge station is less than the first type.

But the area of the construction is greater than required area for first type solar charge station. If the vertical reflectors will be integrated to the second type solar charge station, it will charge more steadily energy than now. The second type solar charge station is shown in Figure 14.

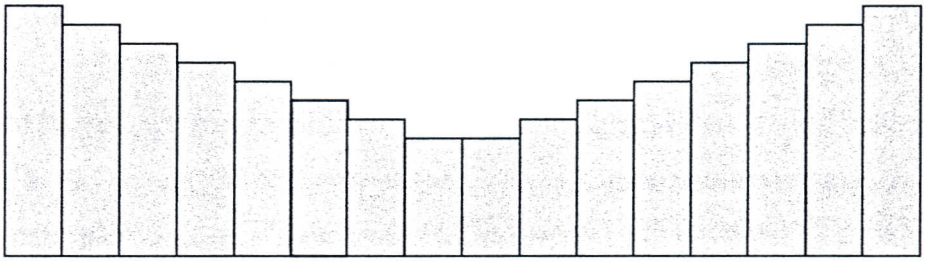

Figure 14: South facing solar charge station with different angles, schematically

7.3. South Facing Solar Charge Station With Fixed Angles (Third Type)

In this type of solar charge station, azimuth angle is equal to zero because of the modules' faces are turned to the south. The latitude of Izmir, $\phi = 38{,}46^0$, therefore, the slope of the modules were taken this value. In Table 7.3, slope of the modules, azimuth angles and calculated values of extraterrestrial solar radiations are given. In the third combination, maximum energy is obtained in March, 622,6096 MJ/m^2 and minimum amount of energy is 459,7696 MJ/m^2 in December.

In Figure 38, first type and third type solar charge station were compared and the amount of the obtained energy in third type is greater than values of first type solar charge station. However the energy gain is more than the first type, the fluctuation of the total energy curve over one year period is the nearly same. In addition to this, the vertical reflectors are integrated to the two systems the energy differences between the systems will not change and the third type will give more energy.

The third type solar charge station is represents in Figure 15, as schematically.

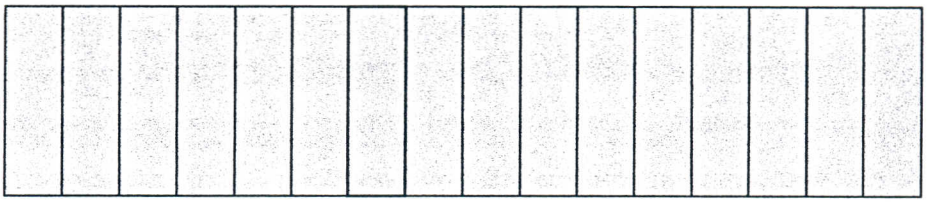

Figure 15: South facing solar charge station with fixed angles, schematically

7.4. Inverse of Omega Type Solar Charge Station (Fourth Combination)

In fourth type solar charge station, slope of the modules, β, were taken inverse of the first type solar charge station's slope of the modules. In Table 7.4 these values are given with azimuth angles and value of solar radiations. In fourth type combination, maximum energy is 573,1266 MJ/m^2 in April and minimum energy is 343,5094 MJ/m^2 in December.

According to the Figure 39, there was no differences between the first type solar charge station and fourth type solar charge station as amount of energy and fluctuation of the curve over one year period.

7.5 Optimisation of South Facing Solar Charge Station with Different Angles (Fifth Combination) and Optimisation of Omega Type Solar Charge Station

According to the obtained values charge more energy with second type solar charge station. That's why, for increasing of the amount of the energy, decided to calculate optimised value for second type solar charge station. Thus, optimum values of slopes, β, and maximum energy amounts for these slopes were found. This type of solar charge station was called as fifth combination.

In this combinations, azimuth angles are zero because face of the modules are turned to south side and slope of the modules are optimised for obtaining maximum energy in each month in fifth combination. In optimisation of first type azimuth angles

are same in omega type solar charge station but slope of the modules are changed for maximum amount of energy. In Table 7.5.1, the values of energy, azimuth angles and optimised slopes of the modules in fifth type solar charge station are given. The maximum energy is 677,056 MJ/m^2 in June and minimum energy is 502,6656 MJ/m^2 in December.

In Table 7.5.2 is given the amount of energy, azimuth angle and optimised slope of the first type solar charge station and they were shown in Figure 21-36 The maximum energy is 668,571 MJ/m^2 in June and the minimum amount of energy is 360,29 MJ/m^2 in December. For the compare fifth types solar charge station with first combination, the optimisation of first type solar charge station were done. In Figure 40, the solar energy gain of the fifth combination were compared collected energy by the first type solar charge station. The amounts of the energy in fifth combination are greater than amounts in first combination. If the vertical reflectors are integrated to the captured reflected beams, the energy gain will increase in fifth type solar charge station.

The optimisation of first type solar charge station we could obtain 5684,52 MJ/m^2 energy in one-year period. But, in fifth type solar charge station, the total energy is 7115,918 MJ/m^2 in one-year period. According to the results, maximum amount of energy is obtained with fifth type solar charge station in Izmir

Chapter VIII

CONCLUSION

Growing world energy consumption forced energy industries to use low quality, dirtier burning coal, to search for oil under the oceans as well as on land and to develop poor hydroelectric or hydropower sites in order to meet the demand for power. Strip mining, flooding from hydroelectric dams and offshore oil spills ruined landscapes and coastlines, while clouds of soot and automobile exhaust in the cites and stockpiles of radioactive waste from nuclear power plants began to pose a serious threat to human life.

The world currently uses fossil fuels 100000 times faster than nature can form them. At present rates of consumption, the remaining untapped sources of fossil fuel can only supply energy for an estimated 170 years. World population statistics indicate, that rates of energy consumption will increase. At the start of industrial revolution the world had only a few hundred million inhabitants. By 1990 the population had increased to 5 billion. Energy demand has risen in step with population growth. Since the end of the 19^{th} century, oil and natural gas consumption has doubled every 15 to 20 years. If the current rate of increase continues only 20% of the world's supply of oil and natural gas will remain by the middle of the 21^{st} century.

Transportation now consumes more than 20% of the world's total primary energy and produces much of the world's air pollution. In just 30 years, the number of cars in the world will soar from today's 400 million or so, to more than one billion. Private transportation will then need 2,5 times more energy and produce 2,5 times more air pollution. If global trends are projected to year 2100, the world will need ten times more total energy and transportation will consume 40% of this required energy.

Today, automobiles operate at approximately 15% efficiency, which means that about 15% of the energy contained in the fuel is delivered to the drive wheels as useful work.

Electric cars produce significantly fewer harmful emissions; they have save about 10% to 30% in primary energy.

The aim of this study is finding suitable solar charge station which is collected maximum amount of solar radiation and fluctuations of collected radiation is less than the others over one year period. According to the results of calculations, 7115,91 MJ/m^2 energy can be obtained from the fifth combination model, which is more suitable than the others are. If amount of energy can be obtained at a higher value in January, February, March, October, November and December, this solar charge station will be most suitable model that shows a stable trend over a year period. For this purpose, vertical reflectors must be integrated to the modules in fifth combination model. In all models, extraterrestrial solar radiations were calculated and shadow calculations were not examined. For more accurate results of calculations, the terrestrial amounts of solar radiations must be calculated with helping of these extraterrestrial solar energy results.

The second phase of this study is installation of modules on the roof and measured the amount of energy as experimentally and calculated values are compared with the measured values.

Omega type solar charge station was located at the roof of the Electrical Engineering Department, in Gülbahçe, in Izmir. Our solar charge station is formed 16 photovoltaic modules and their construction materials are chosen aluminium. The delaying in purchasing and construction of modules, only two set experiments were done. Although the experiments were carried out from 28 June 2000 until 15 October 2000, the measurements on 28 September and 15 October are given in this thesis to the following results are obtained: the total value of the hourly radiation is11, 6812 MJ from 9:00 to 18:00. In the second experiment, at the end of the measuring of data 12,0368 MJ are obtained. But second set was done from 9:00 to 17:00. If the vertical reflectors are integrated to the omega type solar charge station, of course, additional energy gain is obtained. Thus, the amount of the total energy will go a little bit higher.

The meteorological data are found 78,6164 MJ on 28 September and 86,7517MJ on 15 October as direct solar radiation on inclined surfaces. According to these results our system efficiency is found % 13. The efficiency for crystalline silicon solar cells is given in literature between 11 and 13 percent. Thus, we can obtain optimum energy with our system.

But these estimated results are not reliable, because the amounts of the energy were not measured over a year period. And the location of the experimental set-up and

Güzelyalı Meteorological Station are different. The climatic factors, like wind, temperature, cloudiness etc., are very changeable Thus, experimental results and meteorological data are not compared correctly. For optimum result, the amount of the energy must be measured with omega type solar charge station over one year period and they must be compared with another meteorological station data, for example in Urla,

In this study only omega type solar charge station was located, but the amount of the energy were not measured with other types solar charge stations. In the future, other solar charge stations should be settled and total amount of energy must be compared with omega type solar charge station and the meteorological data. Vertical and tilted reflectors should be added to the omega type solar charge station. Measurements should be carried out with these reflectors.

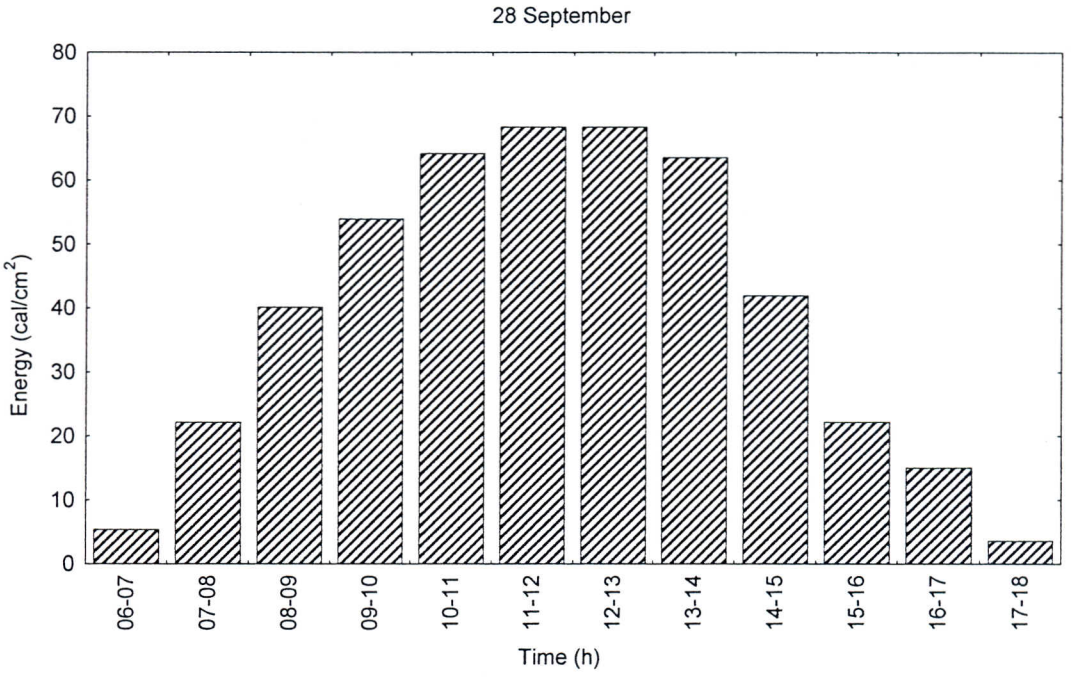

Figure 16: Total Solar Radiations on Horizontal Surface (Meteorological Data on 28 September)

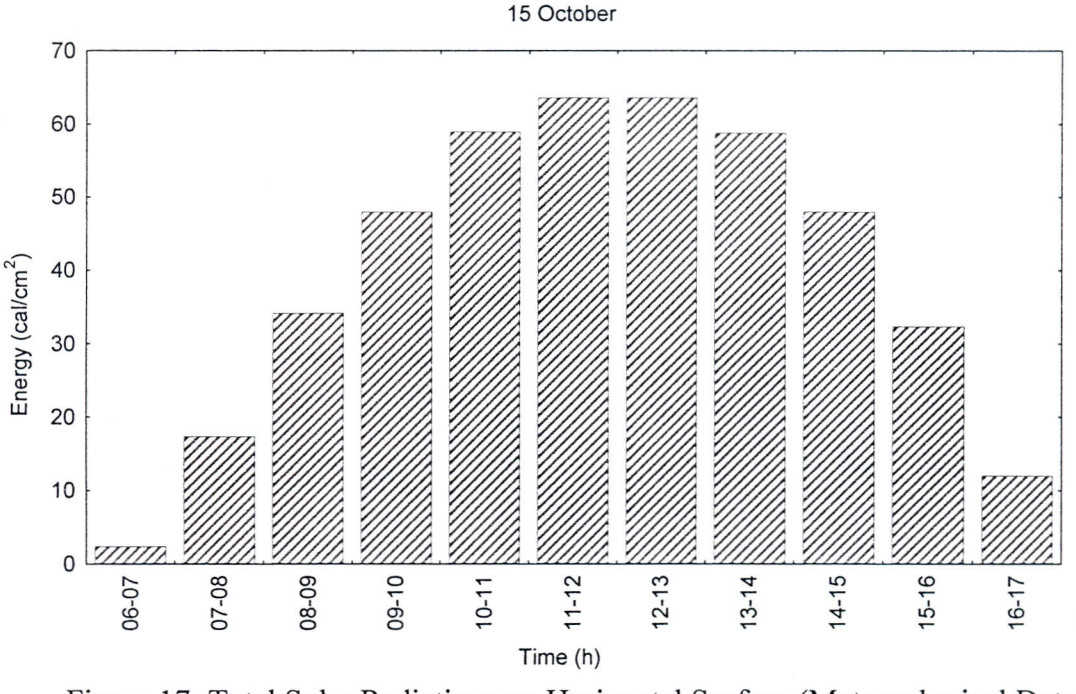

Figure 17: Total Solar Radiations on Horizontal Surface (Meteorological Data on 15 October)

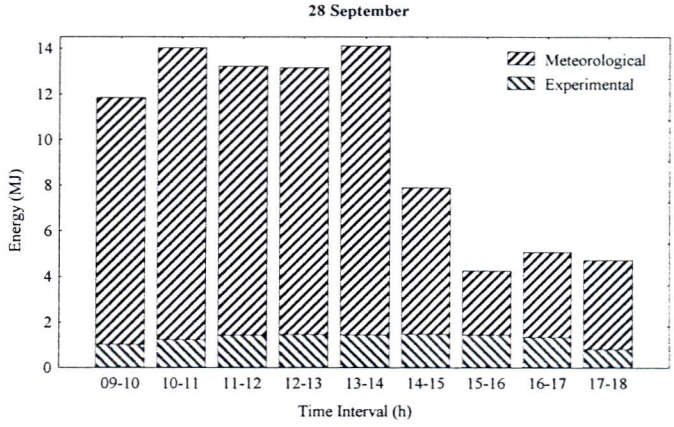

Figure 18: Comparision of Experimental Results and Direct Solar Radiations on Inclined Surfaces from Meteorological Station data on 28 September

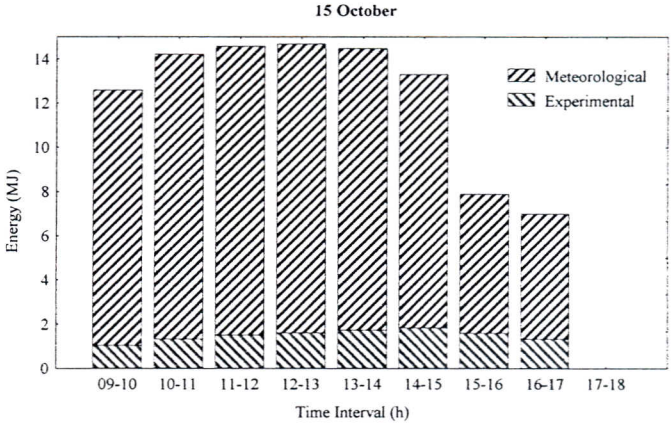

Figure 19: Comparision of Experimental Results and Direct Solar Radiations on Inclined Surfaces from Meteorological Station Data on 15 October

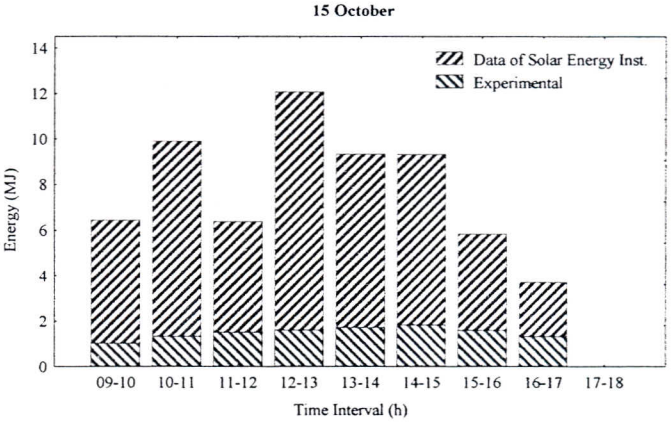

Figure 20: Comparision of Experimental Results and Measured Data of Solar Energy Institute on 15 October

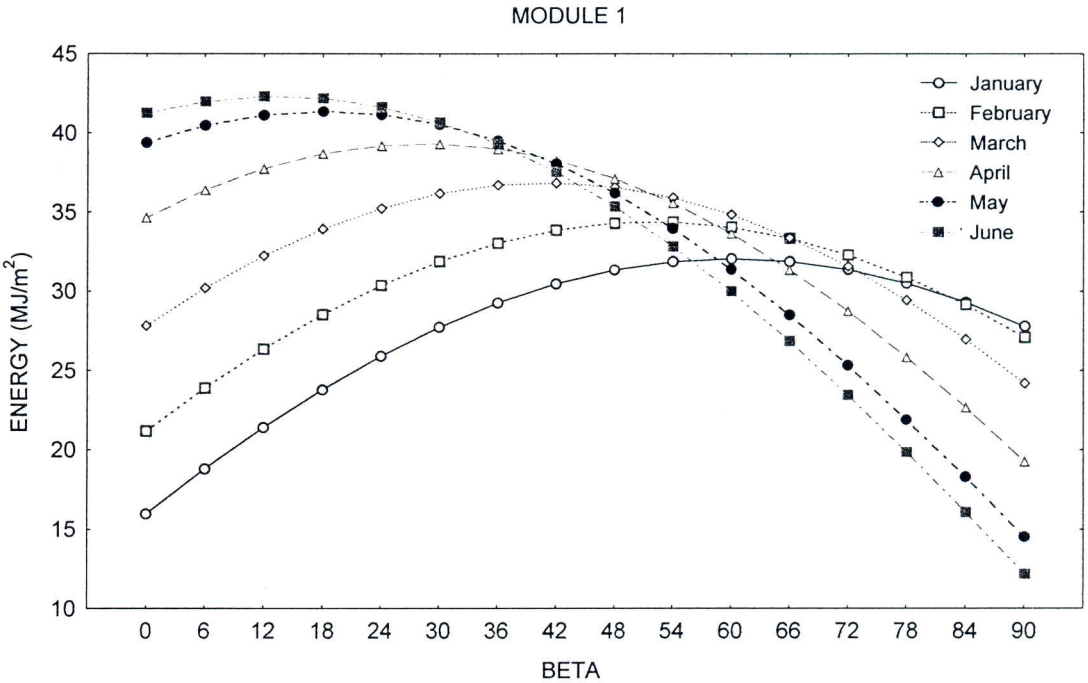

Figure 21: Slope Optimisation of Module 1 in First Type Solar Charge Station for First Six Months

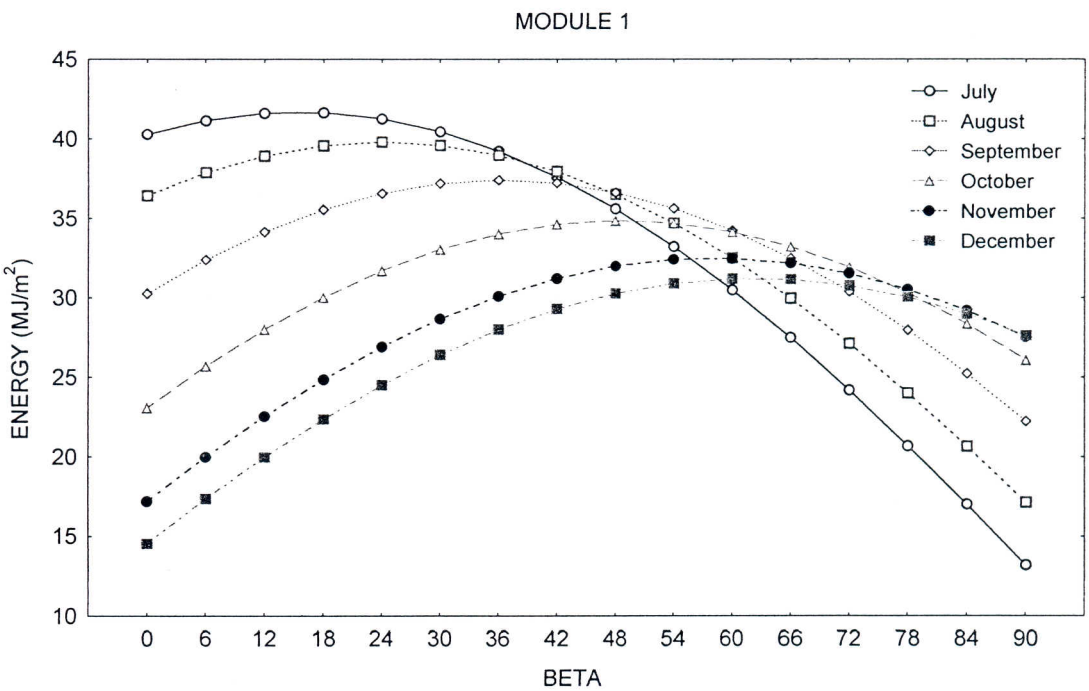

Figure 22: Slope Optimisation of Module 1 in First Type Solar Charge Station for Second Six Months

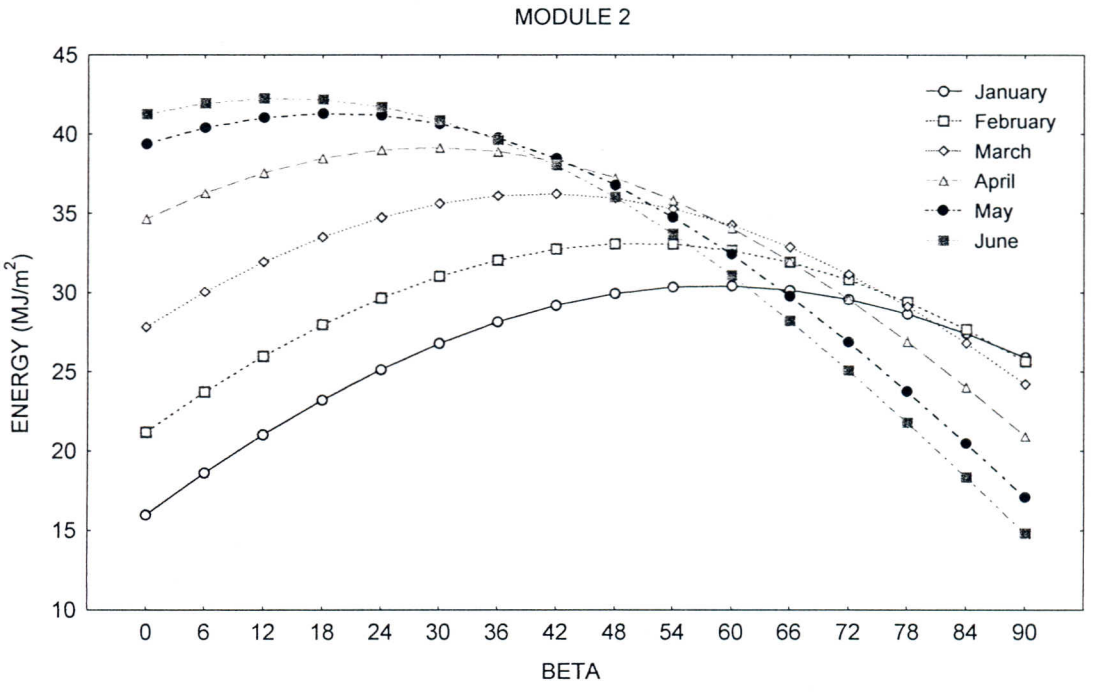

Figure 23: Slope Optimisation of Module 2 in First Type Solar Charge Station for First Six Months

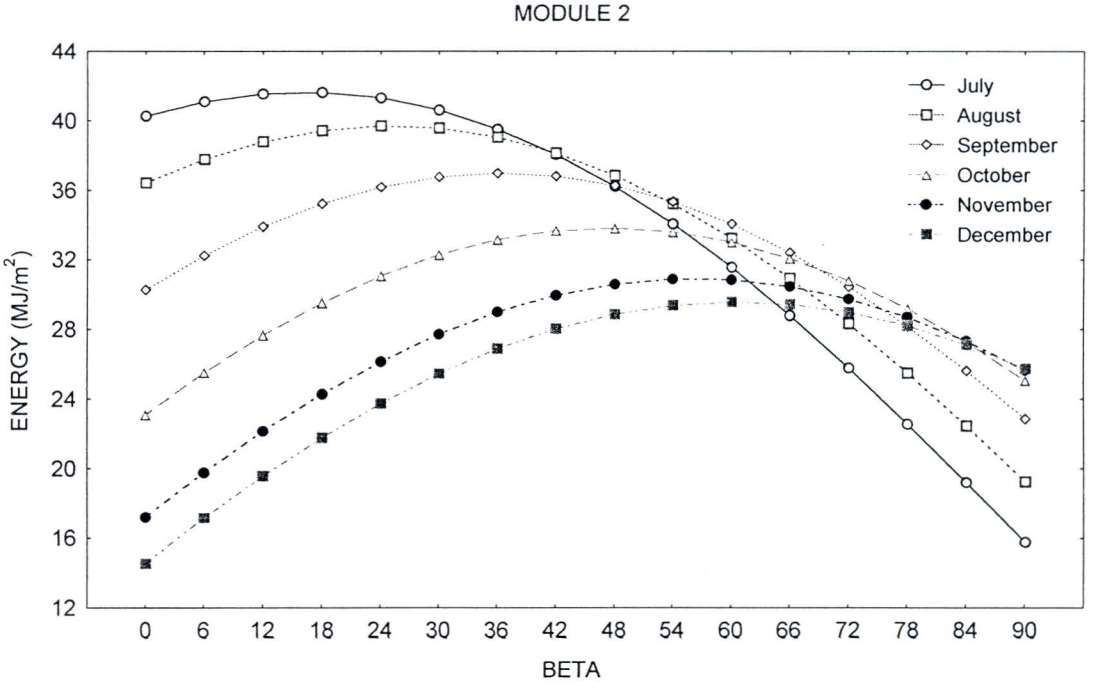

Figure 24: Slope Optimisation of Module 2 in First Type Solar Charge Station for Second Six Months

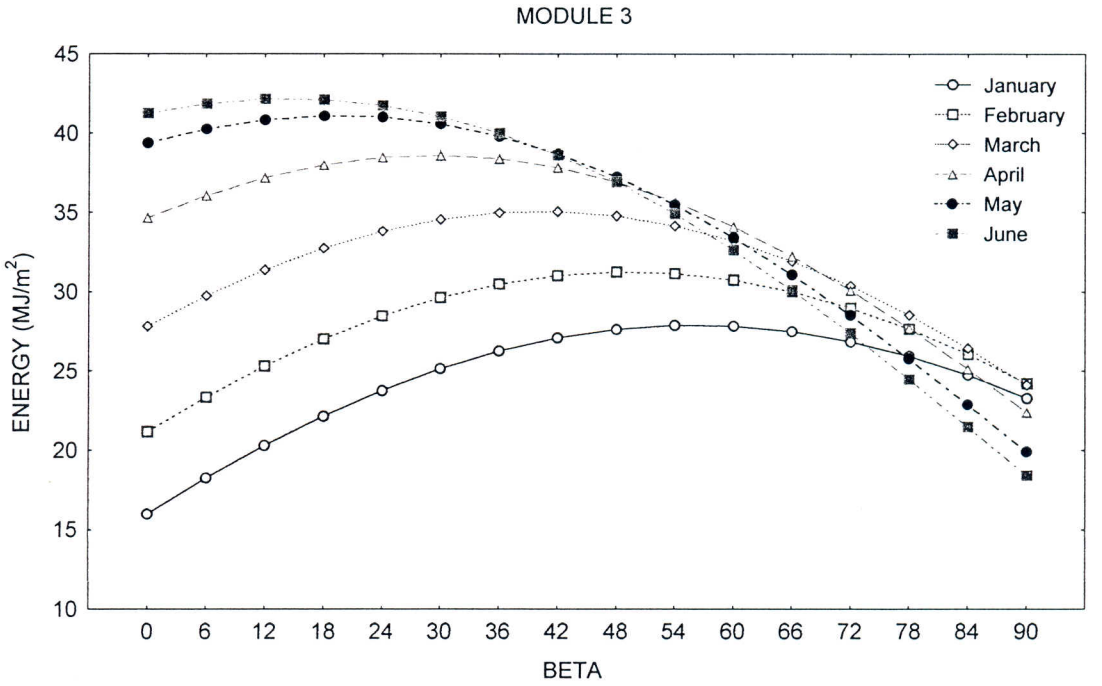

Figure 25: Slope Optimisation of Module 3 in First Type Solar Charge Station for First Six Months

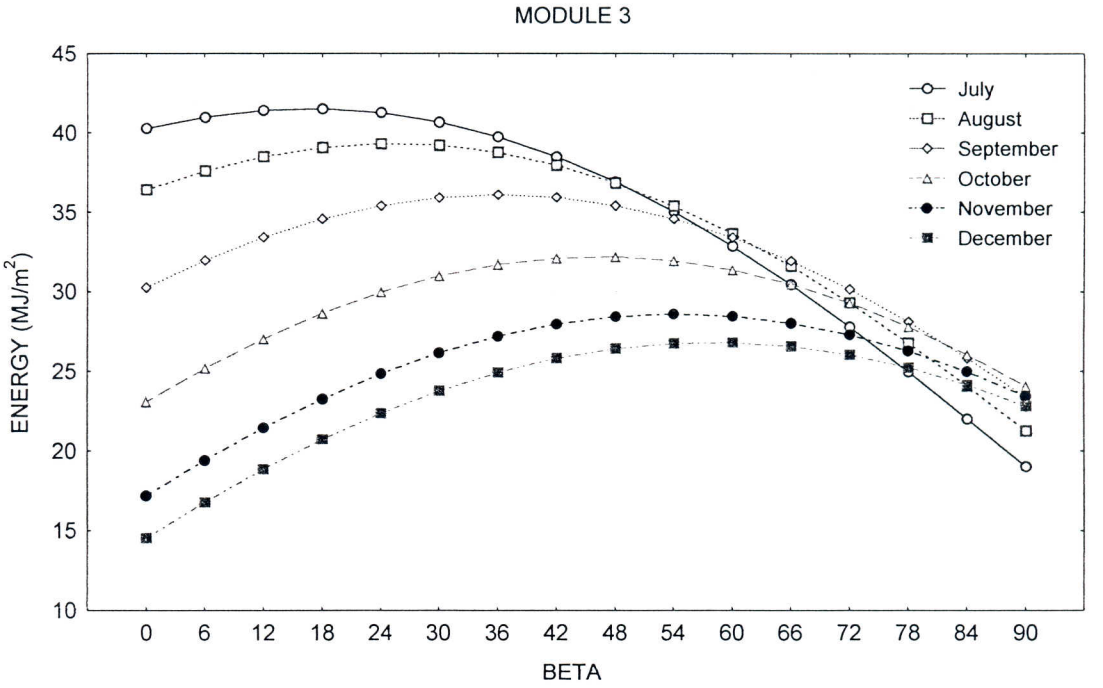

Figure 26: Slope Optimisation of Module 3 in First Type Solar Charge Station for Second Six Months

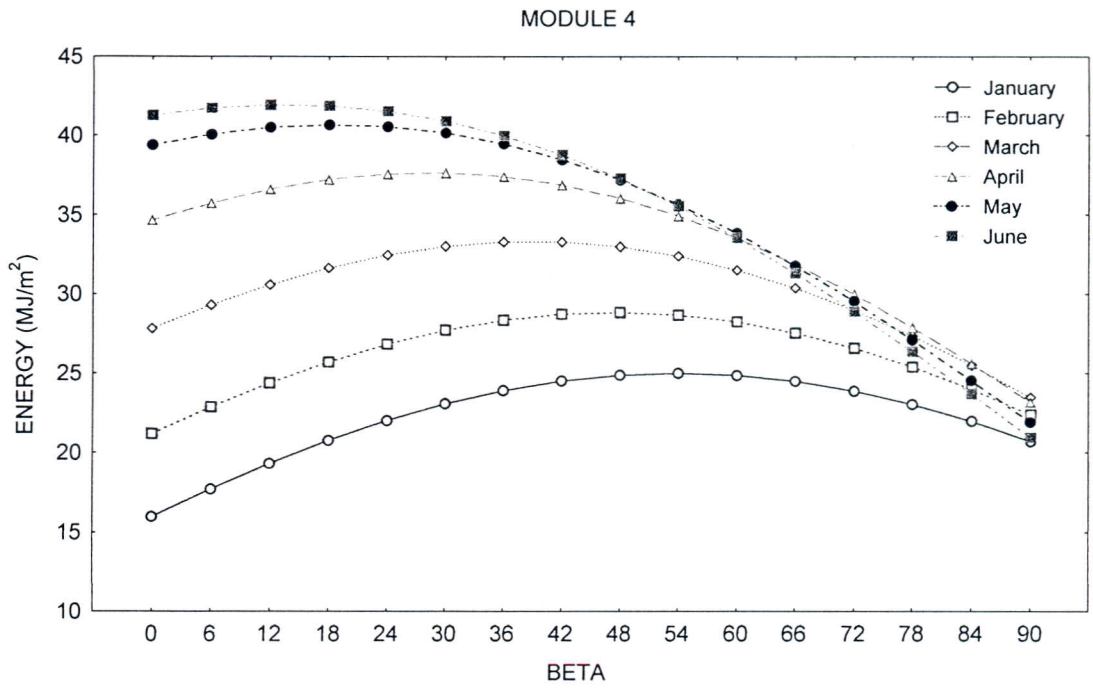

Figure 27: Slope Optimisation of Module 4 in First Type Solar Charge Station for First Six Months

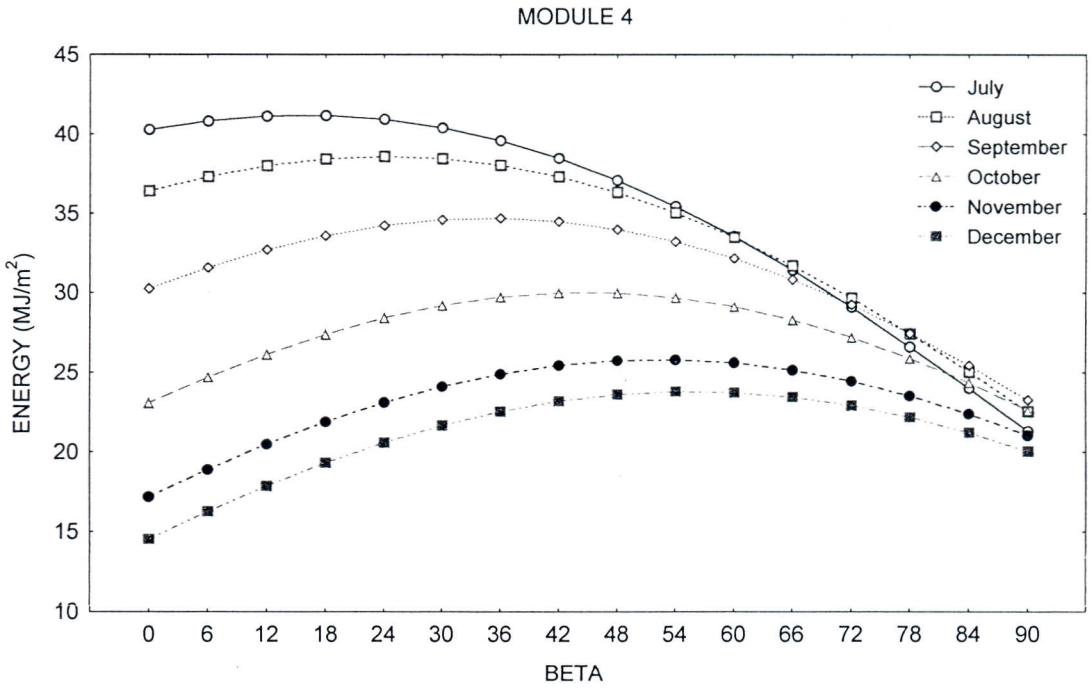

Figure 28: Slope Optimisation of Module 4 in First Type Solar Charge Station for Second Six Months

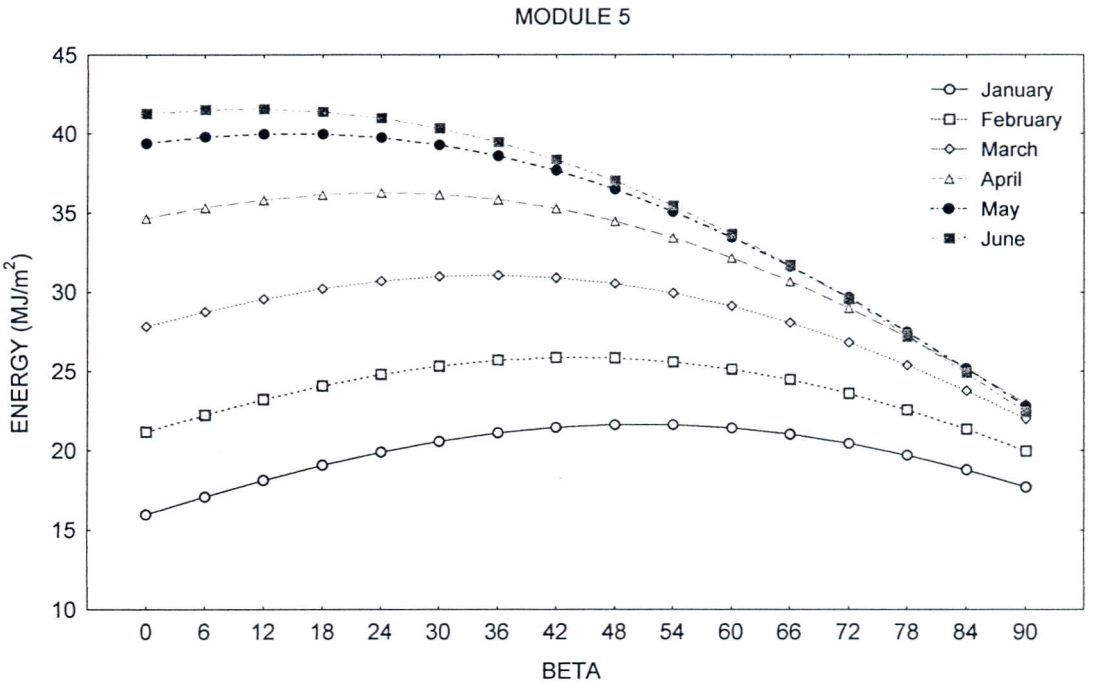

Figure 29: Slope Optimisation of Module 5 in First Type Solar Charge Station for First Six Months

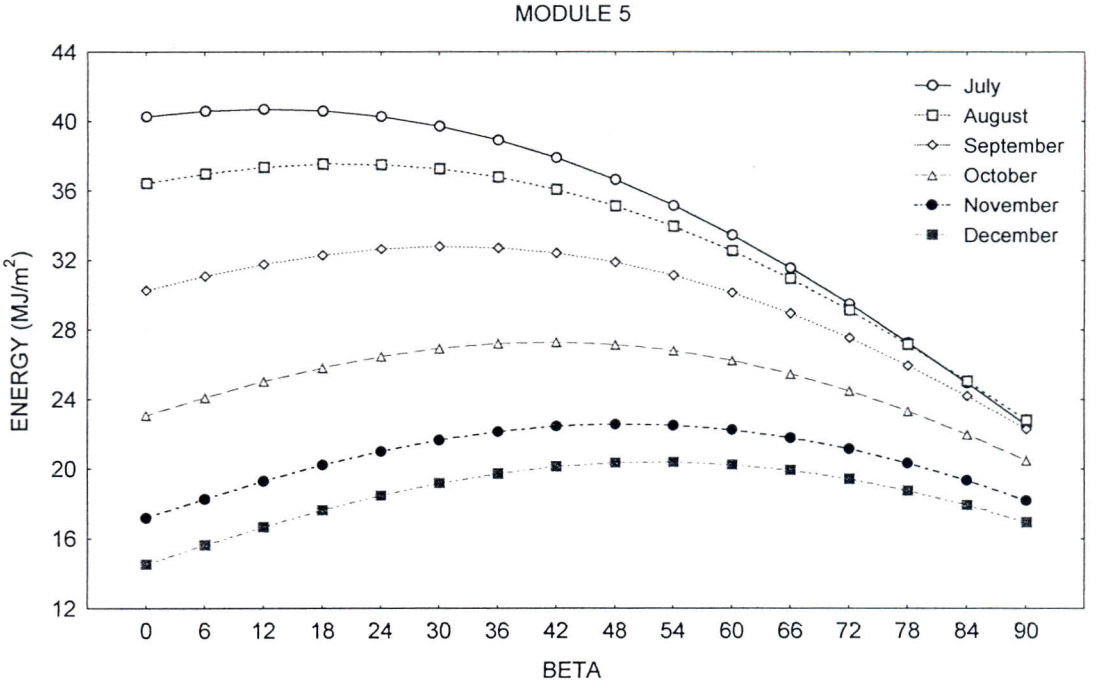

Figure 30: Slope Optimisation of Module 5 in First Type Solar Charge Station for Second Six Months

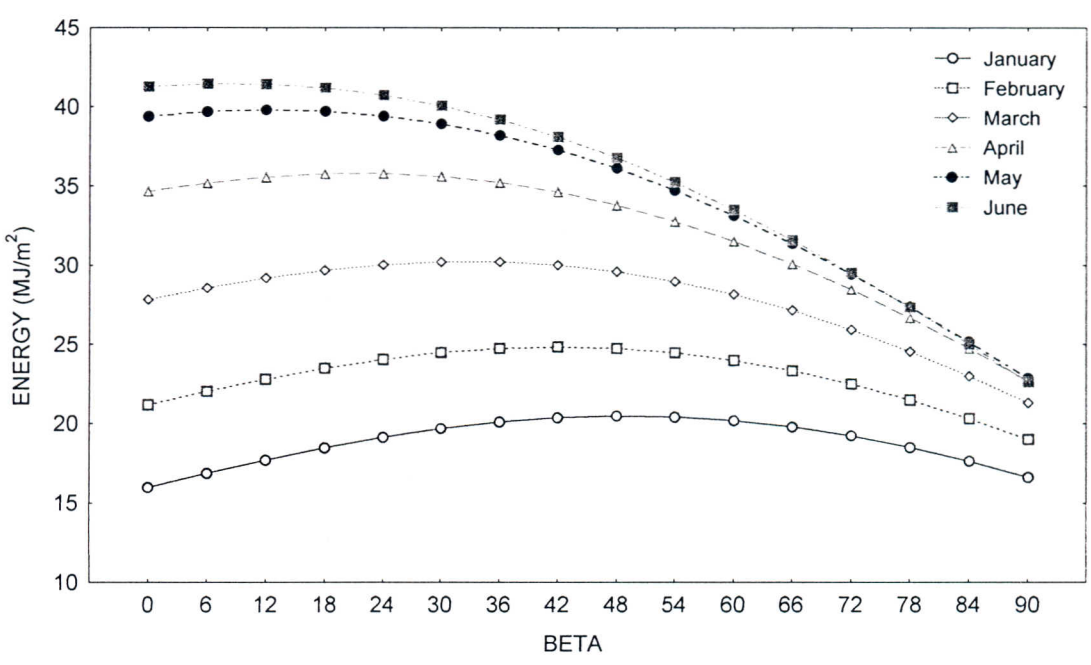

Figure31: Slope Optimisation of Module 6 in First Type Solar Charge Station for First Six Months

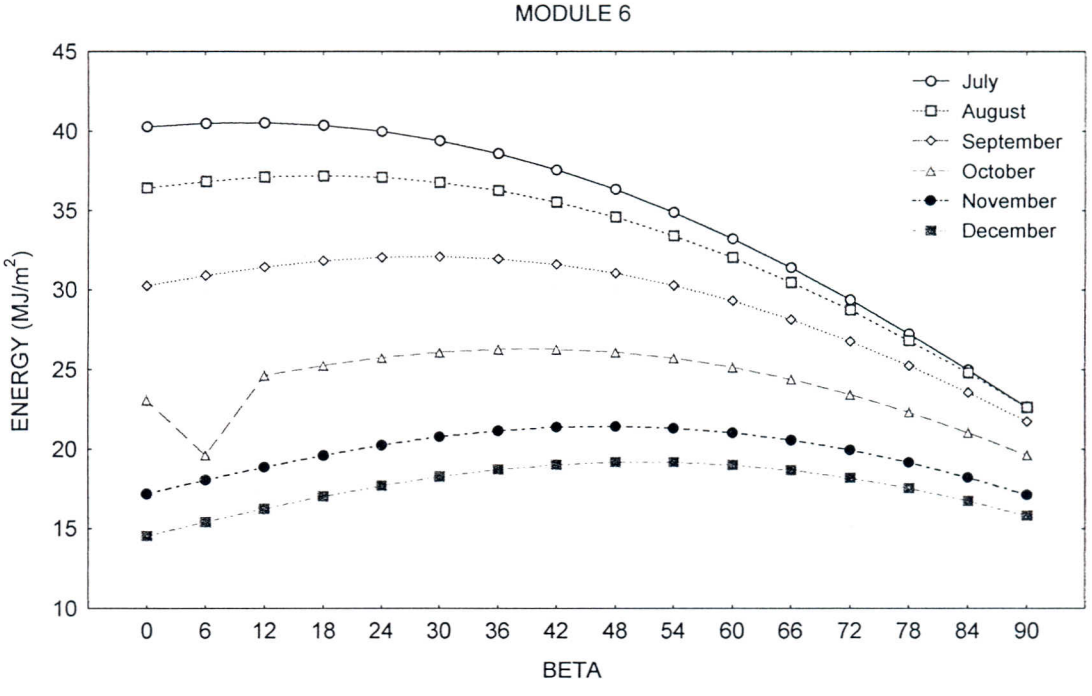

Figure 32: Slope Optimisation of Module 6 in First Type Solar Charge Station for Second Six Months

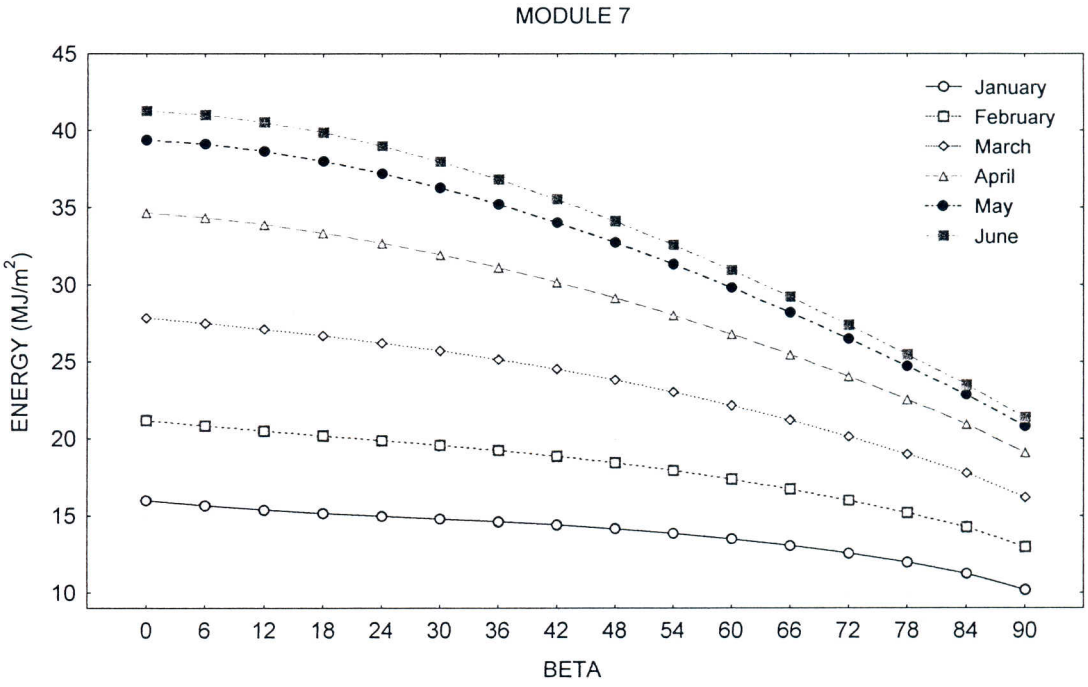

Figure 33: Slope Optimisation of Module 7 in First Type Solar Charge Station for First Six Months

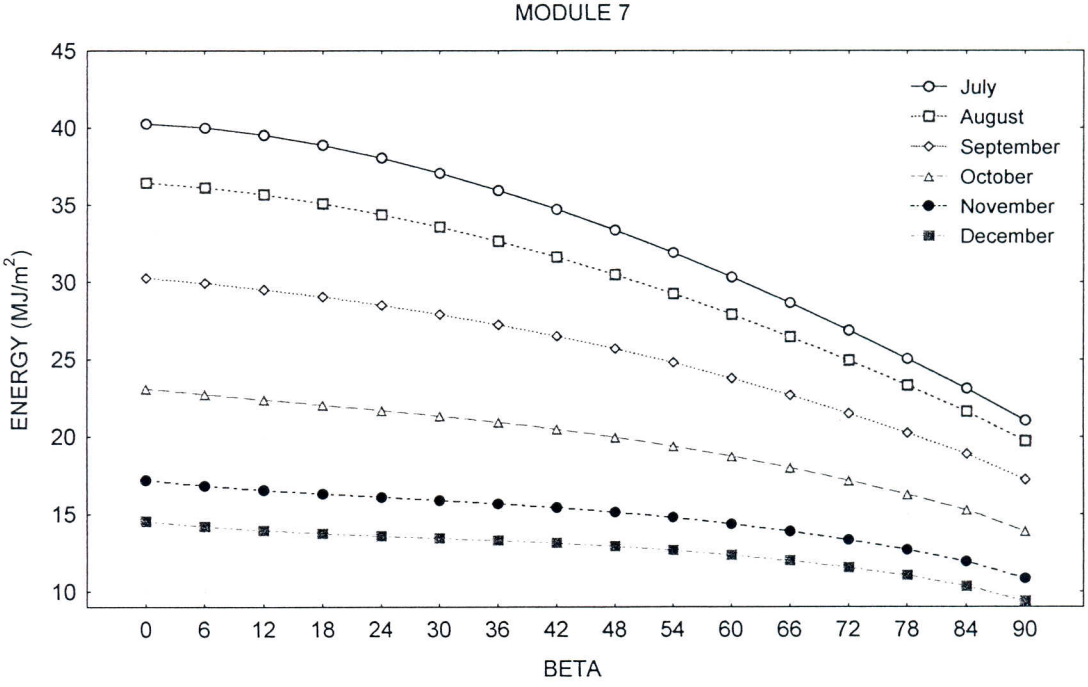

Figure 34: Slope Optimisation of Module 7 in First Type Solar Charge Station for Second Six Months

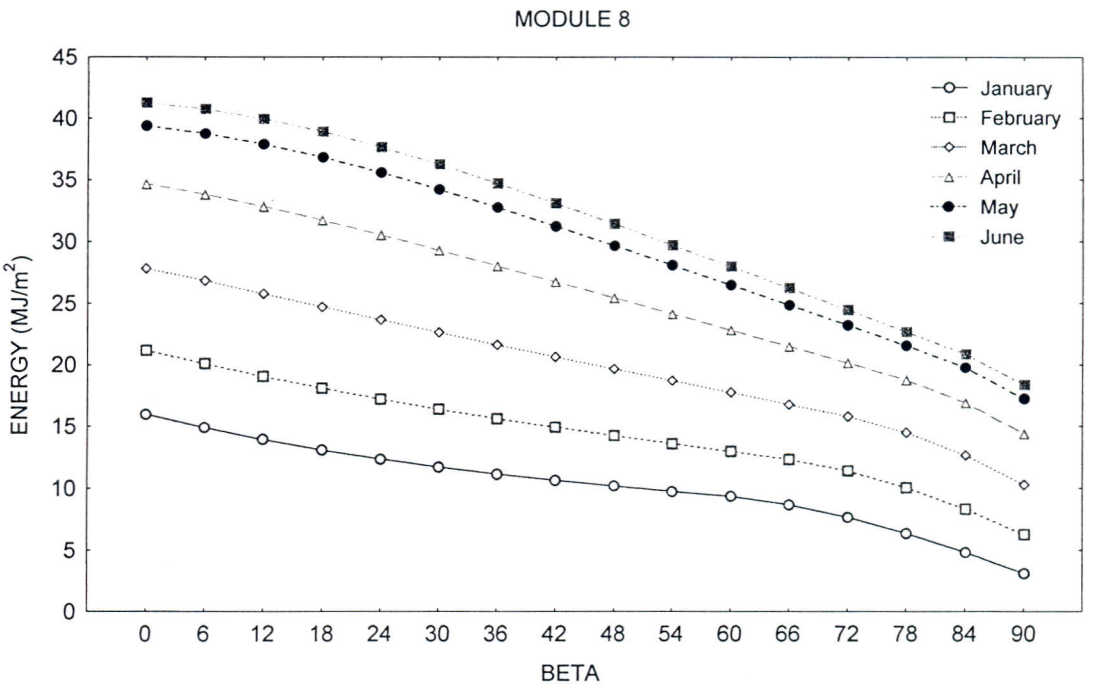

Figure 35: Slope Optimisation of Module 8 in First Type Solar Charge Station for First Six Months

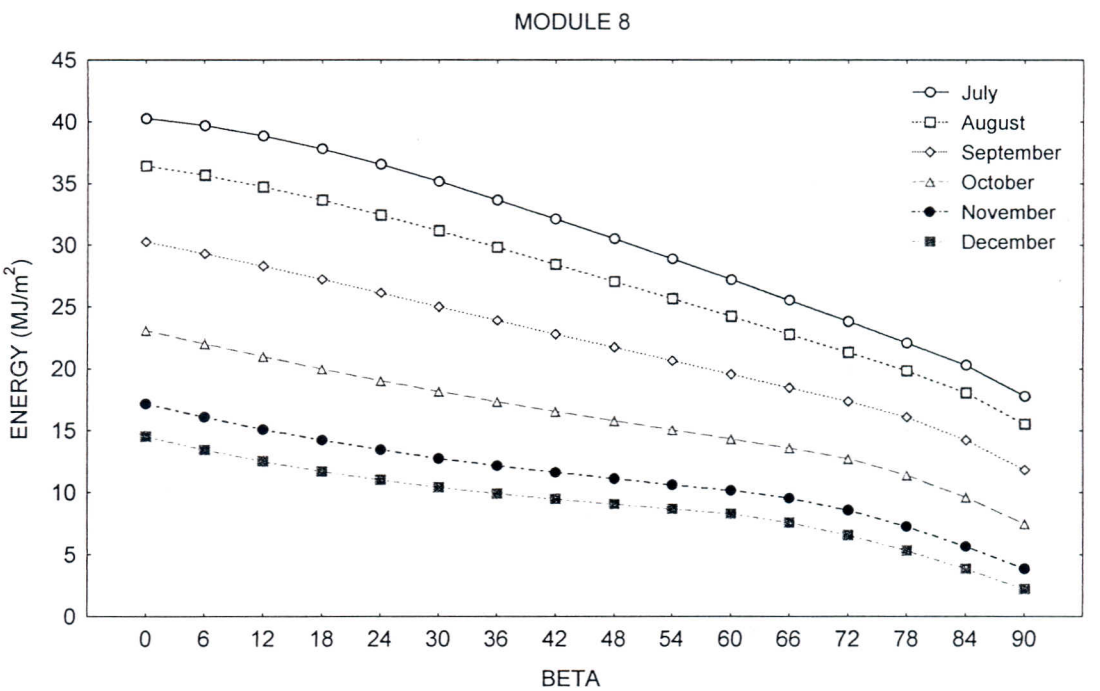

Figure 36: Slope Optimisation of Module 8 in First Type Solar Charge Station for Second Six Months

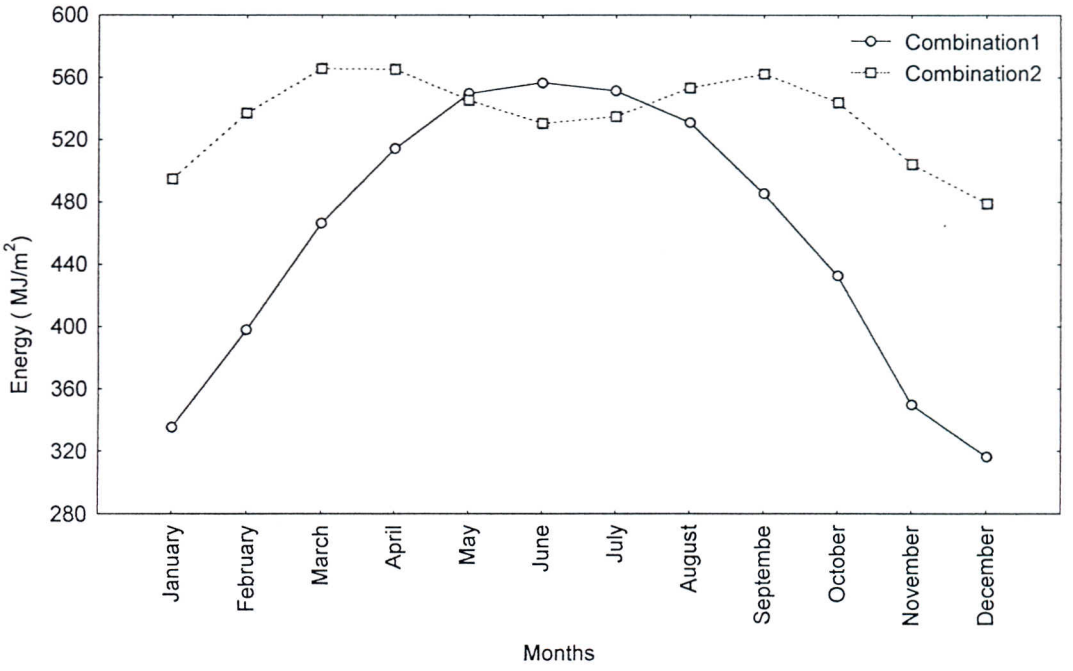

Figure 37:.Comparison of Combination 1 and Combination 2

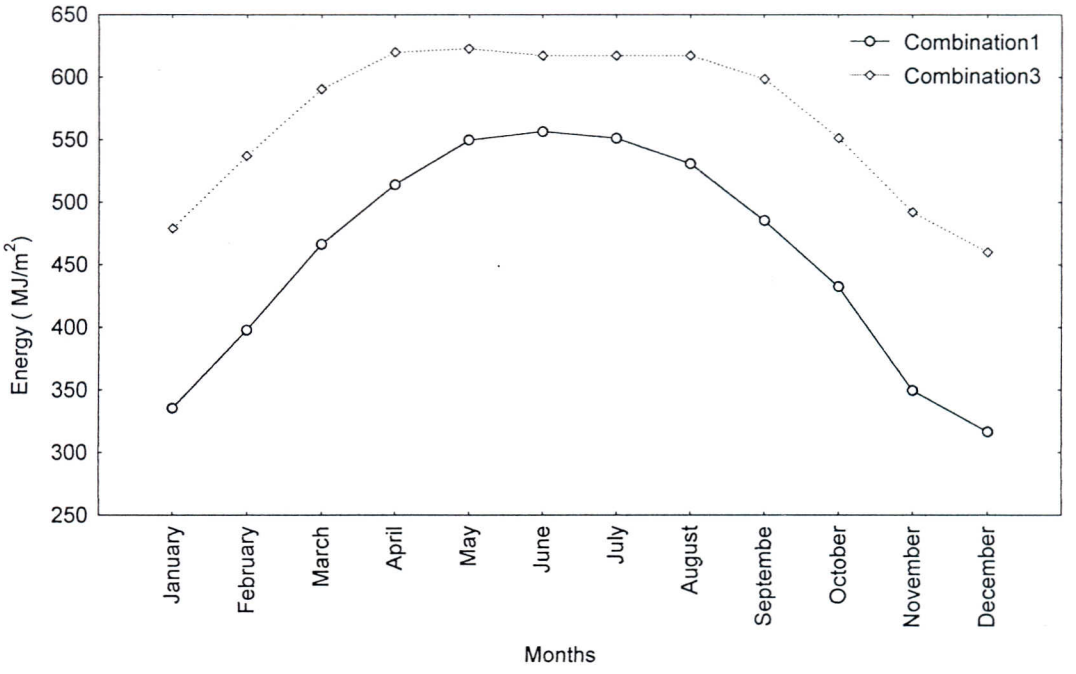

Figure 38: Comparison of Combination 1 and Combination 3

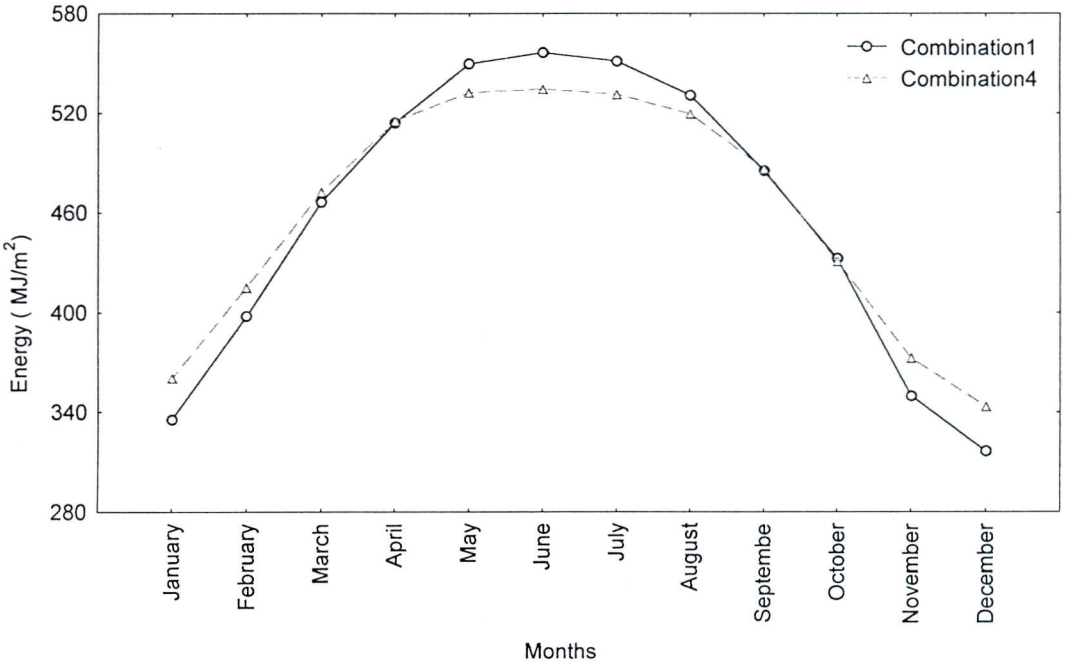

Figure 39: Comparison of Combination 1 and Combination 4

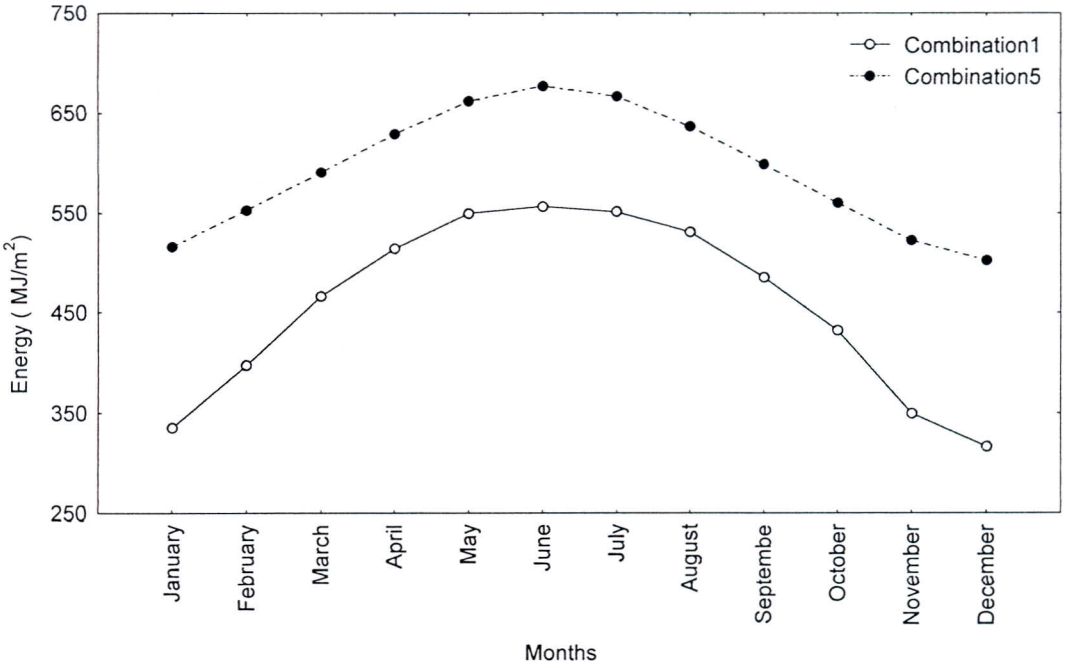

Figure 40: Comparison of Combination 1 and Combination 5

Table 5.4.1: Amount of Direct Solar Radiations on Inclined Surfaces on 28 September 2000, the Meteorological Data (MJ)

	β	γ	09-10	10-11	11-12	12-13	13-14	14-15	15-16	16-17	17-18	Total
Module 1	30	7,5	0,9610	1,1636	1,1278	1,1478	1,2182	0,5835	0,2280	0,2418	0,1371	6,8088
Module 2	36	22,5	0,8231	1,0691	1,0902	1,1590	1,2850	0,6472	0,2709	0,3237	0,2555	6,9237
Module 3	42	37,5	0,6187	0,9064	0,9954	1,1201	1,3070	0,6943	0,3099	0,4067	0,3847	6,7432
Module 4	48	52,5	0,3618	0,6824	0,8424	1,0229	1,2681	0,7125	0,3378	0,4780	0,5073	6,2132
Module 5	54	67,5	0,0738	0,4114	0,6371	0,8659	1,1582	0,6924	0,3481	0,5254	0,6059	5,3182
Module 6	60	82,5	-0,2197	0,1144	0,3918	0,6547	0,9756	0,6286	0,3364	0,5391	0,6651	4,3057
Module 7	66	97,5	-0,4914	-0,1843	0,1240	0,4014	0,7270	0,5208	0,3004	0,5131	0,6738	3,2605
Module 8	72	112,5	-0,7162	-0,4596	-0,1382	0,1232	0,4271	0,3741	0,2411	0,4459	0,6268	2,2382
Module 9	30	-7,5	1,0649	1,2298	1,1478	1,1278	1,1527	0,5265	0,1913	0,1739	0,0145	6,6562
Module 10	36	-22,5	1,1812	1,2972	1,1590	1,0902	1,0591	0,4510	0,1446	0,0899	-0,0742	6,4722
Module 11	42	-37,5	1,2672	1,3194	1,1201	0,9954	0,8979	0,3390	0,0812	-0,0167	-0,2123	6,0201
Module 12	48	-52,5	1,3005	1,2800	1,0229	0,8424	0,6760	0,1983	0,0068	-0,1349	-0,3568	6,3269
Module 13	54	-67,5	1,2637	1,1692	0,8659	0,6371	0,4076	0,0404	-0,0715	-0,2516	-0,4896	4,3839
Module 14	60	-82,5	1,2621	0,9849	0,6547	0,3918	0,1133	-0,1203	-0,1457	-0,3534	-0,5933	3,4068
Module 15	66	-97,5	0,9505	0,7339	0,4014	0,1240	-0,1826	-0,2692	-0,2081	-0,4284	-0,2317	2,2098
Module 16	72	-112,5	0,6827	0,4312	0,2151	-0,1459	-0,4553	-0,3924	-0,2522	-0,4675	-0,6610	1,329
Total	78,6164											

Table 5.4.2: Amount of Direct Solar Radiations on Inclined Surfaces on 15 October 2000, the Meteorological Data (MJ)

	β	γ	09-10	10-11	11-12	12-13	13-14	14-15	15-16	16-17	17-18	Total
Module 1	30	7,5	0,9510	1,1839	1,2746	1,2976	1,2343	1,0562	0,5132	0,3626	-	7,8734
Module 2	36	22,5	0,8223	1,0926	1,2427	1,3220	1,3147	1,0987	0,6193	0,4980	-	8,0103
Module 3	42	37,5	0,6200	0,9294	1,1384	1,2821	1,3425	1,2773	0,7126	0,6310	-	7,9333
Module 4	48	52,5	0,3573	0,6954	0,9600	1,1678	1,2998	1,3086	0,7757	0,7408	-	7,3054
Module 5	54	67,5	0,0558	0,4056	0,7140	0,9774	1,1767	1,2620	0,7937	0,8086	-	6,1938
Module 6	60	82,5	-0,2570	0,0827	0,4161	0,7176	0,9768	1,1285	0,7570	0,8199	-	4,8986
Module 7	66	97,5	-0,5516	-0,2456	0,0883	0,4077	0,6962	0,9101	0,6620	0,7665	-	3,5308
Module 8	72	112,5	-0,7996	-0,5511	-0,2429	0,0668	0,3658	0,6184	0,5123	0,6481	-	2,2114
Module 9	30	-7,5	1,0563	1,2477	1,2976	1,2746	1,1667	0,9509	0,4284	0,2566	-	7,6788
Module 10	36	-22,5	1,1854	1,3282	1,3220	1,2427	1,0815	0,8223	0,3271	0,1325	-	7,4417
Module 11	42	-37,5	1,2774	1,3563	1,2821	1,1384	0,9200	0,6200	0,1836	-0,0310	-	6,7778
Module 12	48	-52,5	1,3087	1,3131	1,1676	0,9600	0,6883	0,3573	0,0099	-0,2172	-	5,8049
Module 13	54	-67,5	1,2621	1,1888	0,9774	0,7140	0,4014	0,0558	-0,1772	-0,4059	-	4,5995
Module 14	60	-82,5	1,1286	0,9825	0,7186	0,4161	0,0819	-0,2570	-0,3583	-0,5752	-	3,3277
Module 15	66	-97,5	0,9101	0,7034	0,4077	0,0883	-0,2431	-0,5515	-0,5144	-0,7051	-	2,1095
Module 16	72	-112,5	0,6184	0,3696	0,0668	-0,2429	-0,5455	-0,7996	-0,6289	-0,7796	-	1,0548
Total	86,7517											

Table 7.1: Omega Type Solar Charge Station (First Type)

Modul No	$\gamma(^{O})$	$\beta(^{O})$	$I_{on\beta}$ (MJ/m^2)											
			January	February	March	April	May	June	July	August	September	October	November	December
1	7.5	30	27.7407	31.8905	36.16666	39.3206	40.5461	40.6948	40.4639	39.6007	37.1867	33.0544	28.6669	26.4208
2	22.5	36	28.1550	32.0666	36.1045	38.9150	39.7551	39.6442	39.5329	39.0595	36.9976	33.1566	29.0029	26.9101
3	37.5	42	27.0942	31.0282	35.0387	37.8351	38.6977	38.6389	38.5130	37.9893	35.9365	32.1189	27.9684	25.8396
4	52.5	48	24.8697	28.8328	32.9798	36.0457	37.2004	37.2985	37.1082	36.3336	33.9918	29.9779	25.7593	23.6254
5	67.5	54	21.6186	25.5980	29.9468	33.4511	35.0985	35.4650	35.1621	33.9591	31.1384	26.8202	22.5219	20.4004
6	82.5	60	17.5785	21.4831	25.9765	29.9404	32.1596	32.8506	32.4125	30.7042	27.3564	22.7648	18.4734	16.4212
7	97.5	66	13.0518	16.71565	21.180	21.4713	28.2088	29.2171	28.6505	26.4716	22.6984	18.0038	13.8976	12.0059
8	112.5	72	7.6692	11.4018	15.8123	20.1591	23.2317	24.4860	23.8267	21.3218	17.3655	20.3981	8.5774	6.5989
9	-7.5	30	27.7407	31.8905	36.16666	39.3206	40.5461	40.6948	40.4639	39.6007	37.1867	33.0544	28.6669	26.4208
10	-22.5	36	28.1550	32.0666	36.1045	38.9150	39.7551	39.6442	39.5329	39.0595	36.9976	33.1566	29.0029	26.9101
11	-37.5	42	27.0942	31.0282	35.0387	37.8351	38.6977	38.6389	38.5130	37.9893	35.9365	32.1189	27.9684	25.8396
12	-52.5	48	24.8697	28.8328	32.9798	36.0457	37.2004	37.2985	37.1082	36.3336	33.9918	29.9779	25.7593	23.6254
13	-67.5	54	21.6186	25.5980	29.9468	33.4511	35.0985	35.4650	35.1621	33.9591	31.1384	26.8202	22.5219	20.4004
14	-82.5	60	17.5785	21.4831	25.9765	29.9404	32.1596	32.8506	32.4125	30.7042	27.3564	22.7648	18.4734	16.4212
15	-97.5	66	13.0518	16.71565	21.180	21.4713	28.2088	29.2171	28.6505	26.4716	22.6984	18.0038	13.8976	12.0059
16	-112.5	72	7.6692	11.4018	15.8123	20.1591	23.2317	24.4860	23.8267	21.3218	17.3655	20.3981	8.5774	6.5989
Total Energy			**335,5554**	**398,0334**	**466,4104**	**514,2766**	**549,7958**	**556,5794**	**551,3396**	**530,8796**	**485,3426**	**438,5894**	**349,7356**	**316,4446**

Table 7.2: South Facing Solar Charge Station with Different Angles (Second Type)

Modul No	$\gamma(^O)$	$\beta(^O)$	$I_{on\beta}$ (MJ/m^2)											
			January	February	March	April	May	June	July	August	September	October	November	December
1	0	30	27.8565	32.0074	36.2905	39.3905	40.5289	40.6687	40.4419	39.5944	37.2227	33.1670	28.7858	26.5401
2	0	36	29.4053	33.1975	36.7946	38.9938	39.4707	39.2723	39.2014	38.9603	37.4323	34.1599	30.2470	28.1572
3	0	42	30.6319	34.0240	36.9356	38.2425	37.9970	37.4715	37.5530	37.9081	37.2321	34.7785	31.3768	29.4658
4	0	48	31.5229	34.4776	36.6719	37.0764	36.1239	35.2857	35.5146	36.4491	36.6241	35.0161	32.1628	30.4516
5	0	54	32.0686	34.5535	36.0065	35.5086	33.8726	32.7395	33.1091	34.5997	35.6151	34.8699	32.5965	31.1037
6	0	60	32.2629	34.2509	34.9466	33.5565	31.2687	29.8622	30.3641	32.3769	34.2162	34.3418	32.6730	31.4151
7	0	66	32.1037	33.5730	33.5038	31.2420	28.3425	26.6877	27.3119	29.8175	32.4427	33.4375	32.3916	31.3822
8	0	72	31.5927	32.5272	31.6939	28.5912	25.1290	23.2547	23.9892	26.9396	30.3141	32.1668	31.7552	31.0056
9	0	30	27.8565	32.0074	36.2905	39.3905	40.5289	40.6687	40.4419	39.5944	37.2227	33.1670	28.7858	26.5401
10	0	36	29.4053	33.1975	36.7946	38.9938	39.4707	39.2723	39.2014	38.9603	37.4323	34.1599	30.2470	28.1572
11	0	42	30.6319	34.0240	36.9356	38.2425	37.9970	37.4715	37.5530	37.9081	37.2321	34.7785	31.3768	29.4658
12	0	48	31.5229	34.4776	36.6719	37.0764	36.1239	35.2857	35.5146	36.4491	36.6241	35.0161	32.1628	30.4516
13	0	54	32.0686	34.5535	36.0065	35.5086	33.8726	32.7395	33.1091	34.5997	35.6151	34.8699	32.5965	31.1037
14	0	60	32.2629	34.2509	34.9466	33.5565	31.2687	29.8622	30.3641	32.3769	34.2162	34.3418	32.6730	31.4151
15	0	66	32.1037	33.5730	33.5038	31.2420	28.3425	26.6877	27.3119	29.8175	32.4427	33.4375	32.3916	31.3822
16	0	72	31.5927	32.5272	31.6939	28.5912	25.1290	23.2547	23.9892	26.9396	30.3141	32.1668	31.7552	31.0056
Total Energy			**494,8890**	**537,2222**	**565,6868**	**565,2030**	**545,4666**	**530,4846**	**534,9704**	**553,2912**	**562,1986**	**543,8750**	**503,9774**	**479,1024**

Table 7.3: South Facing Solar Charge Station with Fixed Angles (Third Type)

Module No	$\gamma(^O)$	$\beta(^O)$	$I_{on\beta}$ (MJ/m^2)											
			January	February	March	April	May	June	July	August	September	October	November	December
1	0	38.46	29.9513	33.5829	36.9017	38.7352	38.9131	38.5785	38.5709	38.5770	37.3994	34.4606	30.7540	28.7356
2	0	38.46	29.9513	33.5829	36.9017	38.7352	38.9131	38.5785	38.5709	38.5770	37.3994	34.4606	30.7540	28.7356
3	0	38.46	29.9513	33.5829	36.9017	38.7352	38.9131	38.5785	38.5709	38.5770	37.3994	34.4606	30.7540	28.7356
4	0	38.46	29.9513	33.5829	36.9017	38.7352	38.9131	38.5785	38.5709	38.5770	37.3994	34.4606	30.7540	28.7356
5	0	38.46	29.9513	33.5829	36.9017	38.7352	38.9131	38.5785	38.5709	38.5770	37.3994	34.4606	30.7540	28.7356
6	0	38.46	29.9513	33.5829	36.9017	38.7352	38.9131	38.5785	38.5709	38.5770	37.3994	34.4606	30.7540	28.7356
7	0	38.46	29.9513	33.5829	36.9017	38.7352	38.9131	38.5785	38.5709	38.5770	37.3994	34.4606	30.7540	28.7356
8	0	38.46	29.9513	33.5829	36.9017	38.7352	38.9131	38.5785	38.5709	38.5770	37.3994	34.4606	30.7540	28.7356
9	0	38.46	29.9513	33.5829	36.9017	38.7352	38.9131	38.5785	38.5709	38.5770	37.3994	34.4606	30.7540	28.7356
10	0	38.46	29.9513	33.5829	36.9017	38.7352	38.9131	38.5785	38.5709	38.5770	37.3994	34.4606	30.7540	28.7356
11	0	38.46	29.9513	33.5829	36.9017	38.7352	38.9131	38.5785	38.5709	38.5770	37.3994	34.4606	30.7540	28.7356
12	0	38.46	29.9513	33.5829	36.9017	38.7352	38.9131	38.5785	38.5709	38.5770	37.3994	34.4606	30.7540	28.7356
13	0	38.46	29.9513	33.5829	36.9017	38.7352	38.9131	38.5785	38.5709	38.5770	37.3994	34.4606	30.7540	28.7356
14	0	38.46	29.9513	33.5829	36.9017	38.7352	38.9131	38.5785	38.5709	38.5770	37.3994	34.4606	30.7540	28.7356
15	0	38.46	29.9513	33.5829	36.9017	38.7352	38.9131	38.5785	38.5709	38.5770	37.3994	34.4606	30.7540	28.7356
16	0	38.46	29.9513	33.5829	36.9017	38.7352	38.9131	38.5785	38.5709	38.5770	37.3994	34.4606	30.7540	28.7356
Total Energy			**479,2208**	**537,3264**	**590,4272**	**619,7632**	**622,6096**	**617,2560**	**617,1344**	**617,232**	**598,3904**	**551,3696**	**492,064**	**459,7696**

Table 7.4: Inverse of Omega Type Solar Charge Station (Fourth Type)

Module No	$\gamma(^{O})$	$\beta(^{O})$	$I_{on\beta}$ (MJ/m^2)											
			January	February	March	April	May	June	July	August	September	October	November	December
1	7.5	72	31.3644	32.3031	31.5789	28.7706	25.3312	23.4661	24.1956	27.1275	30.3812	31.9503	31.5282	30.7790
2	22.5	66	30.1554	31.9168	32.8833	31.9918	29.7842	28.2203	28.7976	30.9210	32.4015	32.0732	30.4581	29.4450
3	37.5	60	27.8327	30.7407	33.2023	34.1093	33.4189	32.6469	32.8643	33.6402	33.4031	31.3649	28.4626	26.8263
4	52.5	54	24.9877	28.6728	32.3916	34.9304	35.6486	35.5451	35.4522	35.0441	33.2107	29.6904	25.8138	23.8133
5	67.5	48	21.6331	25.8475	30.5485	34.4886	36.4980	37.0318	36.6475	35.1398	31.8982	27.1729	22.5939	20.3637
6	82.5	42	18.0524	22.5669	27.9754	33.0573	36.1964	37.3094	36.6637	34.1814	29.7570	24.1144	19.0904	16.7524
7	97.5	36	14.6083	19.2496	25.1382	31.1189	35.2120	36.8312	35.9594	32.6436	27.2585	20.9474	15.6795	13.3232
8	112.5	30	11.7064	16.3958	22.6298	29.3258	34.2093	36.2558	35.1934	31.1816	25.0174	18.2000	12.7897	10.4518
9	-7.5	72	31.3644	32.3031	31.5789	28.7706	25.3312	23.4661	24.1956	27.1275	30.3812	31.9503	31.5282	30.7790
10	-22.5	66	30.1554	31.9168	32.8833	31.9918	29.7842	28.2203	28.7976	30.9210	32.4015	32.0732	30.4581	29.4450
11	-37.5	60	27.8327	30.7407	33.2023	34.1093	33.4189	32.6469	32.8643	33.6402	33.4031	31.3649	28.4626	26.8263
12	-52.5	54	24.9877	28.6728	32.3916	34.9304	35.6486	35.5451	35.4522	35.0441	33.2107	29.6904	25.8138	23.8133
13	-67.5	48	21.6331	25.8475	30.5485	34.4886	36.4980	37.0318	36.6475	35.1398	31.8982	27.1729	22.5939	20.3637
14	-82.5	42	18.0524	22.5669	27.9754	33.0573	36.1964	37.3094	36.6637	34.1814	29.7570	24.1144	19.0904	16.7524
15	-97.5	36	14.6083	19.2496	25.1382	31.1189	35.2120	36.8312	35.9594	32.6436	27.2585	20.9474	15.6795	13.3232
16	-112.5	30	11.7064	16.3958	22.6298	29.3258	34.2093	36.2558	35.1934	31.1816	25.0174	18.2000	12.7897	10.4518
Total Energy			**360,681**	**415,386**	**472,696**	**573,126**	**532,597**	**534,613**	**531,4874**	**519,7584**	**486,6552**	**431,027**	**372,8324**	**343,509**

Table 7.5.1: Optimisation of South Facing Solar Charge Station (Fifth Type)

Months	$\beta(^0)$	$\gamma(^0)$	$I_{on\beta}$ (MJ/m^2)
January	60	0	516,2224
February	54	0	552,8592
March	42	0	590,9696
April	30	0	629,1472
May	18	0	661,7584
June	12	0	677,056
July	18	0	666,4384
August	24	0	636,848
September	36	0	598,9152
October	48	0	560,2608
November	60	0	522,7776
December	60	0	502,6656
Total Energy			**7115,918**

Table 7.5.2: Optimisation of Omega Type Solar Charge Station

Modül		January		February		March		April		May		June	
No	γ	β	$I_{on}\beta$	β	$I_{on}\beta$	β	$I_{on}\beta$	β	$I_{on}\beta$	β	$I_{on}\beta$	β	$I_{on}\beta$
1	7,5	60	32,0563	54	34,3647	42	36,8322	30	39,3201	18	41,3553	12	42,3120
2	22,5	60	30,4166	48	33,0806	42	36,2130	30	39,1640	18	41,3125	12	42,2778
3	37,5	54	27,8824	48	31,2548	42	35,0394	30	38,6131	18	41,1002	12	42,1733
4	52,5	54	24,9877	48	28,8351	36	33,2924	30	37,6302	18	40,6611	12	41,9402
5	67,5	48	21,6331	42	25,8848	36	31,0662	24	36,2837	12	39,9949	12	41,5845
6	82,5	48	20,4646	42	24,8275	30	30,2152	24	35,7746	12	39,7993	6	41,4669
7	97,5	0	15,9921	0	21,1931	0	27,8454	0	34,6708	0	39,3987	0	41,2904
8	112,5	0	15,9921	0	21,1931	0	27,8454	0	34,6708	0	39,3987	0	41,2904
9	-7,5	60	32,0563	54	34,3647	42	36,8322	30	39,3201	18	41,3553	12	42,3120
10	-22,5	60	30,4166	48	33,0806	42	36,2130	30	39,1640	18	41,3125	12	42,2778
11	-37,5	54	27,8824	48	31,2548	42	35,0394	30	38,6131	18	41,1002	12	42,1733
12	-52,5	54	24,9877	48	28,8351	36	33,2924	30	37,6302	18	40,6611	12	41,9402
13	-67,5	48	21,6331	42	25,8848	36	31,0662	24	36,2837	12	39,9949	12	41,5845
14	-82,5	48	20,4646	42	24,8275	30	30,2152	24	35,7746	12	39,7993	6	41,4669
15	-97,5	0	15,9921	0	21,1931	0	27,8454	0	34,6708	0	39,3987	0	41,2904
16	-112,5	0	15,9921	0	21,1931	0	27,8454	0	34,6708	0	39,3987	0	41,2904
Total Energy			**378,85**		**441,27**		**516,7**		**592,25**		**646,041**		**668,671**

Modül		July		August		September		October		November		December	
No	γ	β	$I_{on}\beta$	β	$I_{on}\beta$	β	$I_{on}\beta$	β	$I_{on}\beta$	β	$I_{on}\beta$	β	$I_{on}\beta$
1	7,5	18	41,6513	24	39,7979	36	37,4012	54	34,8491	60	32,4676	60	31,2101
2	22,5	18	41,6369	24	39,7092	36	36,9978	48	33,8088	54	30,8856	60	29,5793
3	37,5	18	41,5088	24	39,3213	36	36,1049	42	32,1206	54	28,6001	60	26,8263
4	52,5	18	41,1672	24	38,6010	36	34,6879	42	29,9945	54	25,8138	54	23,8133
5	67,5	12	40,7072	18	37,5510	30	32,7994	42	27,3092	48	22,5939	54	20,4041
6	82,5	12	40,5403	18	37,1983	30	32,0973	42	26,2973	48	21,4411	48	19,1944
7	97,5	0	40,2784	0	36,4370	0	30,2655	0	23,1102	0	17,1914	0	14,5598
8	112,5	0	40,2784	0	36,4370	0	30,2655	0	23,1102	0	17,1914	0	14,5598
9	-7,5	18	41,6513	24	39,7979	36	37,4012	54	34,8491	60	32,4676	60	31,2101
10	-22,5	18	41,6369	24	39,7092	36	36,9978	48	33,8088	54	30,8856	60	29,5793
11	-37,5	18	41,5088	24	39,3213	36	36,1049	42	32,1206	54	28,6001	60	26,8263
12	-52,5	18	41,1672	24	38,6010	36	34,6879	42	29,9945	54	25,8138	54	23,8133
13	-67,5	12	40,7072	18	37,5510	30	32,7994	42	27,3092	48	22,5939	54	20,4041
14	-82,5	12	40,5403	18	37,1983	30	32,0973	42	26,2973	48	21,4411	48	19,1944
15	-97,5	0	40,2784	0	36,4370	0	30,2655	0	23,1102	0	17,1914	0	14,5598
16	-112,5	0	40,2784	0	36,4370	0	30,2655	0	23,1102	0	17,1914	0	14,5598
Total Energy			**655,537**		**610,11**		**541,24**		**461,2**		**392,37**		**360,29**

REFERENCES

1. Alsema E., Bauman A. E., Hill R., Patterson M. H., "Health, Safety and Environmental Issues in Thin Film Manufacturing", 2nd World Conference on Photovoltaic Solar Energy Conversion, July 1998.
2. Atagündüz G., "Güneş Enerjisi Temelleri ve Uygulamaları" pp:2- 1989
3. Atagündüz G., "Photovoltaic Charge station on Garage Roofs With Passive Reflectors", First Trabzon International Energy and Environment Symposium, vol:2, pp:145-152, 1996
4. Ayres R. U., Frankl P., "Toward a Nonpolluting Energy System", Journal of Environmental Science and Technology V:32, issue:17, pp:408A-410A, September 1998
5. Butler, J., "Environmental Geology, The Solar Solution to Electrical Energy Needs", University of North Caroline at Charlotte, spring semester, 1998
6. Dickinson W. C., Cheremisinoff P.J., "Solar Energy Technology Hand Book" Part A: Engineering Fundamentals, pp.4-6,484, 1980
7. El-Wakil M.M., "Power Plant Technology", pp: 53, 1984.
8. Firester A. H., "Development of Amorphous Silicon Solar Cells", Sun World, V:6, No:3, pp:60-62, 1982
9. Giroult-Matlakowski, G., Theden, U., Blakers, A.W., "In Proceedings of the 2nd World Conference on PV Solar Energy Conversion", pp:3403-3406, 1998
10. Iqbal M., "An Introduction to Solar Radiation", pp: 10- 1983
11. Karl W. Böer, "Advances in Solar Energy" American Solar Energy Society V:7, pp:19-25, 1992
12. Konish N., "Photovoltaics Market Charges up to Make Money", Electronic Design, V:46, issue:25, pp:64C. February 1998
13. Kreider J.F., Hoogendoorn C.J., Kreith F., "Solar Design Components Systems Economics" , pp: 318-320, 1989
14. Kreith F., Kreider J.F., "Principles of Solar Engineering" , pp:37-39, 1978
15. Kreith F., Kreider J. F., "Solar Heating and Cooling: Active and Passive Design", pp: 19- 25, 1982
16. Kulsum A., "Renewable Energy Technologies" A Review of the status and costs of selected technologies The international bank for Reconstruction and Development. pp:47-80

17. Lunde P.J., "Solar Thermal Engineering", pp: 62-, 1980
18. Mclntosh K. R., Koschier L. M., Koh E., Chen P. Y., Quek D., Cotter J. E., Hansberg C. B., "Lowering the Cost of Buried Contact Solar cell Technology", Photovoltaic Special Research Center, 1997
19. Moore T., "High Hopes for High Power Solar", EPRI Journal, pp:16-25, December 1992
20. Morimoto H., Izu M., "In Amorphous semiconductor Technologies and Devices" Japan Annual Review in Electronics, Computers and Telecommunications, pp:212, 1987
21. NASA, National Aeronautics and Space Administration, George C. Marshall Space Flight Center, July 1991
22. Pasachoff J.M., Observatory H., College W., "Electricity from the Sun" , Astronomical Society of the Pacific, V:20, pp:67, 1991
23. Pimentel D., Rodrigues G., Wane T., Abrams R., Goldberg K., Staecker H., Brueckner L., Ma E., Trovato L., Chow C., Gavindarajulu U., Boerke S., "Renewable Energy: Economic and Environmental Issues", Bioscience, V:44, No:8, September 1994
24. Pytlinski, J.T., "Photovoltaic Cell Technologies" University of Puerto Rico Center for Energy and Environment Research, San Juan, pp: 329-334, 1987, Alternative Energy Sources VII, Solar Energy 2
25. Shah A., Torre P., Tscharner R., Wyrsch N., Keppner H., "Photovoltaic Technology :The Case for the Thin-Film Solar Cells" American Association for the Advancement of science, V: 285 (5428), pp: 692-698, July 1999
26. The ABC is of Alternative Fueled Vehicles-A guide to alternative fuel vehicles, pp: 33-39
27. Witt C.E. Eds.,"In Proceedings of the 1st IEEE World Conference on PV Conversion (Institute of Electrical and Electronics Engineers), pp: 2262-2270, 1994
28. Wolfe P.R., Jansen S.W., "In Proceedings on PV solar Energy Conversion" Diretorate General Joint Research Center, pp:1901-1905, 1998
29. World Energy Council Turk National Committee's Journal, December 1993